Development of a Forced Advection Sampling Technique (FAST) for Quantification of Methane Emissions from Orphaned Wells

Mohit L. Dubey[1], Andre Santos[2], Andrew B. Moyes[2], Ken Reichl[2], James E. Lee[3], Manvendra K. Dubey[3], Corentin LeYhuelic[4], Evan Variano[1], Emily Follansbee[3], Fotini K. Chow[1], Sébastien C. Biraud[2]

[1] Department of Environmental Engineering, University of California, Berkeley, CA, 94720, USA

[2] Lawrence Berkeley National Laboratory, Berkeley, CA, 94720, USA

[3] Los Alamos National Laboratory, Los Alamos, NM, 87545, USA

[4] Ecole Normale Supérieure Paris Saclay, Paris, France

Correspondence to: Mohit L. Dubey (mldubey96@berkeley.edu)

Abstract.

Orphaned wells, meaning unplugged and non-producing wells lacking responsible owners, pose a significant and undersampled environmental challenge due to their vast number and unknown associated emissions. We propose, develop, and test an alternative method for estimating emissions from orphaned wells using a Forced Advection Sampling Technique (FAST) that can overcome many of the limitations in current methods (cost, accuracy, safety). In contrast to existing ambient Gaussian plume methods, our approach uses a fan-generated flow to force advection between the emission source and a point methane (CH_4) sensor. The fan flow field is characterized using a colocated sonic anemometer to measure the 3D wind profile generated by the fan. Using time-series measurements of CH_4 concentration and wind, a simple estimate of the CH_4 emission rate of the source can be inferred. The method was calibrated using outdoor controlled release experiments and then tested on four orphaned wells in Lufkin, TX, and Osage County, OK. Our results suggest that the FAST method can provide a low-cost, portable, fast and safe alternative to existing methods with reasonable estimates of orphaned well emissions over a range of leak rates below 40 g/h and within certain geometric and atmospheric constraints.

1 Introduction

1.1 Motivation

Orphaned oil and gas wells, meaning unplugged and non-producing wells lacking responsible owners, pose a significant and undersampled environmental challenge. In the United States (U.S.) alone, there are approximately 120,000 documented orphaned wells [Merrill et al., 2023], with an estimated 310,000 to 800,000 more undocumented wells [IOGCC, 2021]. For much of the 20th century, orphaned wells were considered a non-issue compared to active wells, as they were thought to have low emission rates, particularly when they were reported as "plugged". However, existing estimates of total orphaned well emissions are based only on direct measurements of <0.03% of known wells [Kang et al., 2023], making them a highly undersampled and uncertain source of anthropogenic methane (CH_4). CH_4 is a potent greenhouse gas with a global warming potential (GWP) 84 times higher than carbon dioxide (CO2) taken over 20 years [IEA] and a relatively short

lifetime (8-11 yrs) making it a high priority in combating near-term global warming. Based on a database of leak measurements at 598 wells across the U.S. and Canada, it was found that "annual methane emissions from abandoned wells are underestimated by 150% in Canada and by 20% in the U.S." [Williams et al., 2021]. This lack of reliable emission data has resulted in increased interest in measuring and plugging orphaned wells as an important area of research for methane emissions reduction and near term climate change mitigation.

Alongside academia, the political sphere has shown increased interest in measuring and plugging orphaned wells. The Global Methane Pledge was signed at COP26 in 2021 by 155 countries representing over 50% of global CH_4 emissions who committed to 30% reductions of emissions from 2020 levels by 2030 [UNFCCC Secretariat, 2022]. The U.S. has since begun to investigate plugging orphaned wells, with an investment of $660 million in 2023 through the Department of Interior [DOI, 2023]. From 2018-2020, the average cost of plugging a single well in the U.S. ranged from $2,400 to $227,000, with an overall three-year average of $25,634 [IOGCC, 2021]. Using these numbers directly, without adjusting for inflation or overhead costs, this funding would be sufficient for plugging around 25,000 wells, or only 20% of the documented orphaned wells and a mere 3% of the upper bound of total orphaned wells. Given the high-cost of surveying and plugging, it will be critical to prioritize wells with larger emissions to reduce the economic burden of plugging orphaned wells.

Estimating emissions from orphaned wells is challenging due to their remote locations and typically low emission rates. Based on the aforementioned database of 598 wells across the U.S. and Canada, it has been estimated that orphaned well emission rates range from less than 1 to 48 g/h per well, with an average of around 6 g/h [Williams et al., 2021]. However, recent measurements in the US have also shown abandoned orphaned well emissions exceeding 1 kg/h with a mean value of 138 g/h [Follansbee et al., 2024, Riddick et al., 2024]. Still, extremely high-emitting orphaned wells are very rare and the vast majority of wells emit below the thresholds needed to observe them using current remote sensing platforms [Sherwin et al., 2024].

There are a variety of ground-based measurement approaches that can be applied to measure emissions from orphaned wells (Table 1). These range from expensive hand-held forward looking infrared cameras (FLIR) to more time-intensive mobile (OTM-33a) [U.S. EPA, 2014] and stationary systems (SEMTECH Hi-Flow 2 [SEMTECH], Chamber [Williams et al. 2023], Gaussian Plume Modeling (GPM) [Lushi and Stockie, 2010], Vent [Ventbusters, 2023]). Unmanned aerial vehicles (UAV, also known as "drones") have also recently been proposed as a means of measuring wells, and preliminary results look promising [Dooley et al., 2024]. However, due to the expensive or complex nature of most of these methods only <0.03% of orphaned wells have been sampled. To overcome this data gap, new robust and fast techniques for estimating emission rates on the order of 1-10s g/h are needed (i.e. FAST).

2

Previous studies have investigated existing methods for quantifying methane emissions on the order of those relevant for studying orphaned wells [Dubey et al., 2023, Riddick et al., 2023, 2022]. Table 1 shows a list of the existing technologies that can measure methane emissions in this regime and their relative costs and sensitivities. The existing methods that are accurate and portable enough for measuring orphaned wells have other limitations, including insensitivity (FLIR), high-cost (SEMTECH), complexity and safety (Chamber [Riddick et al., 2023], Vent [Ventbusters, 2023], UAV [Dooley et al., 2024], OTM-33a [Edie et al., 2020]), accuracy, hardware and labor costs that are summarized in Table 1. Therefore, there is a pressing need for a cost-effective, efficient, safe and accurate method using existing sensors to estimate methane emissions for prioritizing orphaned well plugging. Although the FAST method is currently relatively expensive and difficult to set up/transport, it could be considered safer than many approaches, will work in complex aerodynamic environments, and could be used to quantify emissions from larger pieces of infrastructure such as abandoned pump jack wells that won't fit in a chamber or are surrounded by trees.

Method	FLIR Camera	SEMTECH HI-Flow 2	Static Chamber	Dynamic Chamber	GPM	Vent	UAV	OTM-33a	FAST
Hardware Cost	>$50K	~$40K	>$400	>$400	>$5K	~$50K	>$50K	>$10K	$50K*
Range (g/h)	N/A	<1-30,000	>0.1	>0.1	>100	>100	>50	>50	>1
Uncertainty	N/A	±10%	-50%, +100%	±15%	±40%	N/A	N/A	±70%	±50%
Size (L)	~0.3	~15	~20	~20	~50	N/A	~40	>1,000	~50
Measuring Time (min.)	~2	~3	>30	>30	>10	>30	>30	>10	~3
Setup Time (min.)	~5	~5	>10	>10	>10	>10	>30	>30	~30

Table 1: Comparative assessment of commercial (FLIR, SEMTECH Hi-Flow 2, Vent) and research (Chamber, GPM, UAV, OTM-33a) methods used to monitor fugitive methane leaks from orphaned wells. Hardware costs, detection range, accuracy, size, labor and safety are compared for each technology. *The FAST method in this study is currently limited by the high cost of laser trace gas sensors (Picarro, Aeris, etc.) that can be reduced significantly by using cheaper non-laser sensors (i.e. Gas Rover) used in chambers. **The size and setup time of the FAST method can also be decreased

In this paper, we propose, develop, and test a novel method for estimating CH_4 emissions from orphaned wells using a Forced Advection Sampling Technique (FAST) that can overcome many of the limitations of other methods, as outlined in Table 1. In contrast to existing ambient Gaussian plume methods (GPM), our approach uses a fan-generated flow to force advection between the emission source and a point sensor. This eliminates the need for an estimate of atmospheric stability, which is required to use the GPM. Using a colocated anemometer to measure the 3D wind profile generated by the fan, a simple estimate of the CH_4 emission rate of the source can be obtained. The method is calibrated using an outdoor controlled release experiment and blindly tested on four wells in Lufkin, TX, and Osage County, OK. We report results that suggest that the FAST method can potentially provide a low-cost, portable, fast and safe alternative to existing methods to provide reasonable estimates of orphaned well emissions under reasonable meteorological conditions.

## 1.2 Mathematical Model

The physics underlying the FAST approach is based on a steady-state solution to the advection-diffusion equation. This solution, known as the Gaussian plume equation [Veigele and Head, 1978] has been widely used in the literature to perform emission inversions. However, previous studies using the Gaussian plume equation consider larger emission sources and length scales (> 2 meters) than those of interest in this study [Snoun et al., 2023] [Perry et al., 2005]. As a result, traditional GPM studies are typically dependent on parametrizations (i.e. Pasquill stability class), which are too coarse for the length and time scales used when studying orphaned wells at smaller (on the order of a meter) length scales. Furthermore, most previous studies using the GPM approach use ambient winds as opposed to a fan-generated plume within an ambient background. In one exception to this, an approach to localize emissions using a fan-generated flow was devised by [Sanchez-Sosa et al., 2018]. However this approach was only tested indoors and did not estimate emissions for their source of interest (ethanol).
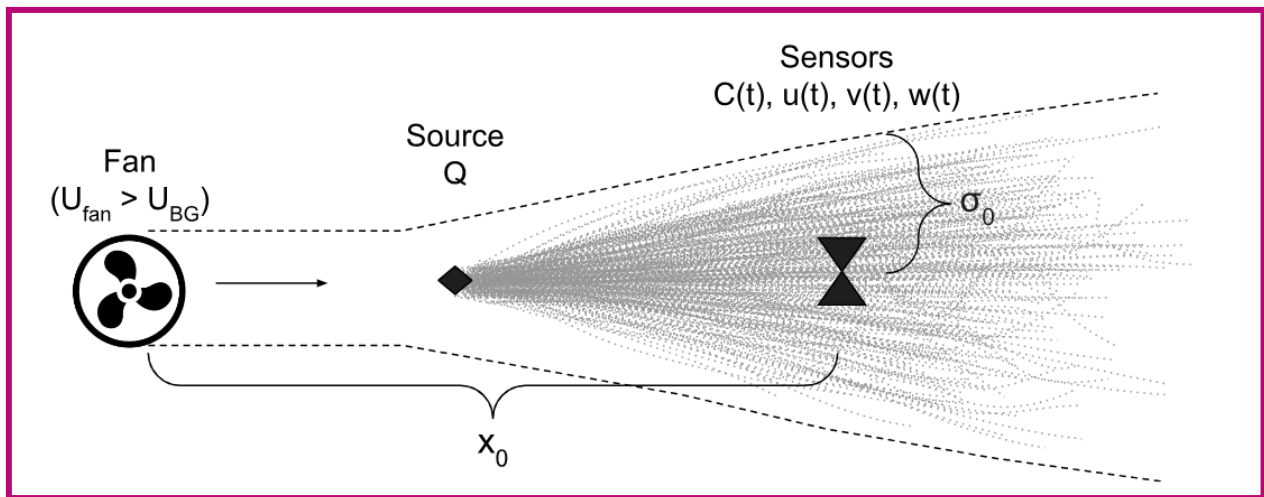
Here we outline the underlying physics of scalar transport within a jet of fan-generated turbulent flow and derive a linear equation that can be used to estimate the emission rate of a source from time-averaged centerline measurements of concentration and wind velocity within that flow.
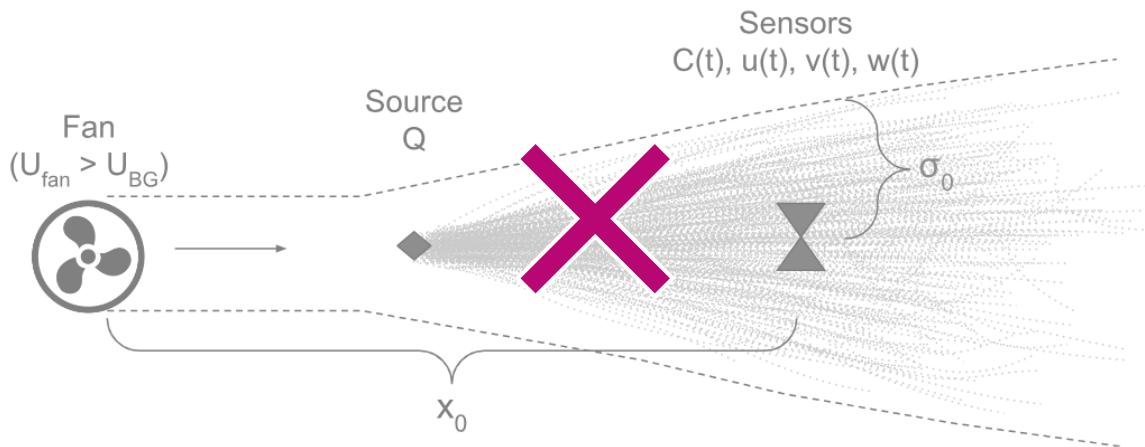
Figure 1: Schematic of the FAST method where an upwind fan (with mean downwind speed U_{fan} larger than the background U_{BG}) generates a turbulent jet to advect a non-reactive gas (CH_4) leaking at volumetric flow rate (Q) from a source to downwind sensors (anemometer measuring u(t), v(t), w(t) and CH_4 analyzer measuring C(t)).

The method assumes a constant emission source with emission rate Q (g/s) positioned downstream from a fan aligned with the mean background wind direction, where the velocity of the fan flow (U_{fan}) is larger than that of the background wind (U_{BG}). Adding this fan creates an environment which is assumed to have homogeneous turbulence between the source and the sensors. The sensors are positioned downstream along the centerline from the fan by a distance (x_0) and measure time series of concentration (C) and velocity (u, v, w).

126   The estimated emission rate ($\hat{Q}$) is calculated by integrating the scalar flux (C•u) over a circular cross-section (dA)

127 at some downstream location.

128
$$Q = \oint C \, u \, dA \approx \underline{C}_{CL} \, \underline{u}_{CL} \, \pi \, \sigma_0^{\,2}$$

129
$$\hat{Q} = \underline{C}_{CL} \, \underline{u}_{CL} \, \pi \, \sigma_0^{\,2} \qquad\qquad (1)$$

130

131 where spatial averages of concentration and velocity are approximated with time averages (underline) of centerline

132 measurements (subscript "CL"). This gives a radial distance (σ_0) which is approximately the effective width of the plume at

133 the downwind distance x_0. This radial distance σ_0 is estimated based on a previous study of fan-generated flows [Halloran et.

134 al, 2014] as a form of turbulent transport [Taylor, 1922]. Halloran et al. showed that the expansion of a fan-generated plume

135 close to the source is proportional to the square root of the downwind distance and dependent on the turbulence intensity

136 (i_{fan}) and characteristic length scale (l_{fan}) of the fan:

137

138
$$\sigma \sim (i_{fan} \, l_{fan} \, x)^{\frac{1}{2}}$$

139
$$\sigma_0 = (\beta \, i_{fan} \, l_{fan} \, x_0)^{\frac{1}{2}} \qquad\qquad (2)$$

140

141 Evaluating Equation 2 at location x_0 and combining with Equation 1, $\hat{Q}$ can be rewritten as a linear function of time-averaged

142 centerline concentration and velocity measurements:

143

144
$$\hat{Q} = \pi \, \beta \, i_{fan} \, l_{fan} \, x_0 \, \underline{C}_{CL} \, \underline{u}_{CL} = K_{FAST} \, \underline{C}_{CL} \, \underline{u}_{CL} \qquad\qquad (3)$$

145

146 where the proportionality constant (K_{FAST}) is only dependent on constants related to the fan and the geometry of the system β

147 (which is treated in more detail in Appendix A):

148

149
$$K_{FAST} = \pi \, \sigma_0^{\,2} = \pi \, \beta \, i_{fan} \, l_{fan} \, x_0 \qquad\qquad (4)$$

150

2 Methods

2.1 Fan Characterization Experiments

To characterize the effectiveness of using a fan to generate a turbulent jet for the FAST method, experiments were conducted at Lawrence Berkeley National Lab (LBNL) on the afternoon of 4/16/2024 and in the morning of 5/21/2024 (Figure 2). For both experiments, a Gill Windmaster (United Kingdom) 3-D sonic anemometer was used to collect 3-D wind speed measurements at 10 Hz downwind of a Minneapolis Duct Blaster (MDB) fan with no attachments. This fan was chosen as it is similar to those used in Halloran et al. and can be easily operated in the field at multiple fan speeds controlled by a dial. Both the fan and the anemometer were mounted on tripods at a height of 1 meter. For these experiments, u is aligned to be in the x direction (upwind/downwind), v in the y direction (crosswind) and w in the z direction (vertical).

A key assumption of this study is that the effective plume width $(\theta\sigma_0)$ derived in Halloran et al. (2014) for smoking oil plumes is applicable to methane dispersion from orphaned wells. While the MDB fan generates turbulent transport similar to Halloran et al., differences in the physical properties of smoking oil and methane—such as buoyancy, diffusion rates, and emission dynamics—could lead to deviations in plume behavior. These potential differences underscore the need for additional experiments designed specifically for methane to validate the use of $(\theta\sigma_0)$ under these conditions and further refine the FAST method's applicability.

During the first experiment, measurements were taken for nine-minute intervals at downwind distances of 0.5 - 5 meters for two different fan speed settings, referred to as "Low" (~3 m/s on average at a distance of 1 m) and "High" (~5 m/s on average at a distance of 1 m). The system was set up to be aligned to the background wind of ~3 m/s from West-NorthWest. Despite attempts to align the fan with the dominant background wind direction, there were still persistent crosswind gusts on the order of ~1 m/s which varied as the experiment progressed. Moreover, the vertical velocity (w) was higher than expected for two main reasons: the anemometer is mounted at a height of 1 meter and the experiment was conducted on a rooftop. While w should be ~0 m/s at ground level, we measured w on the order of ~1 m/s due to these factors.

Experiment 1 (4/16/2024)

Experiment 2 (5/21/2024)

176
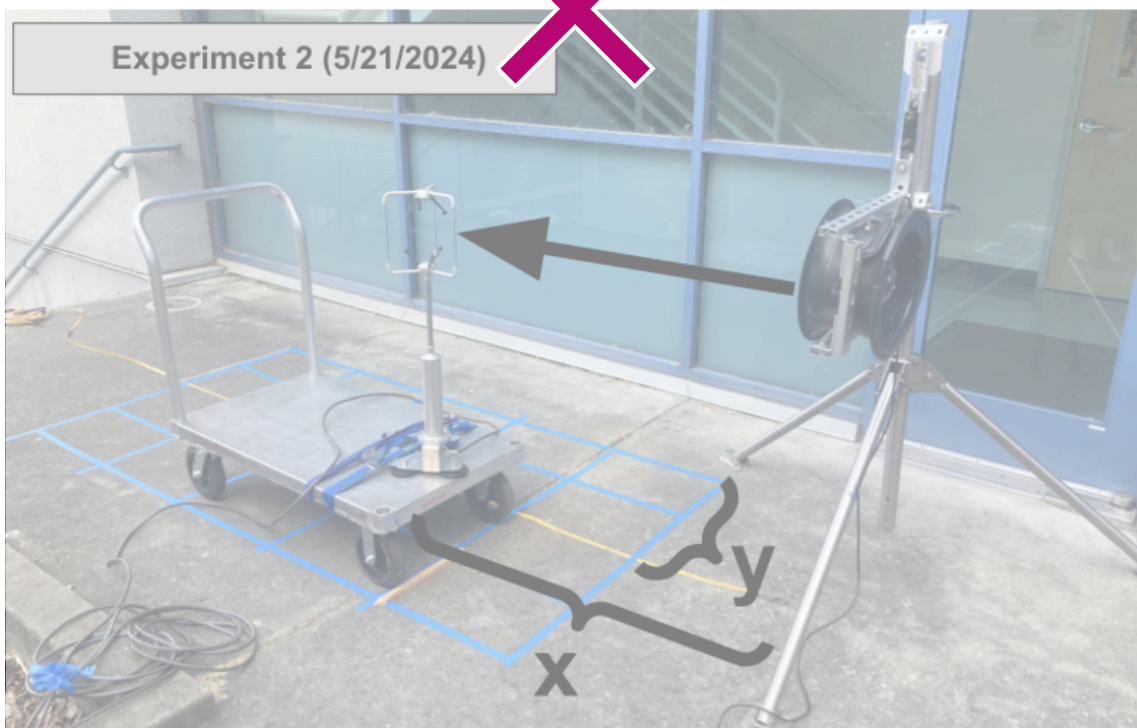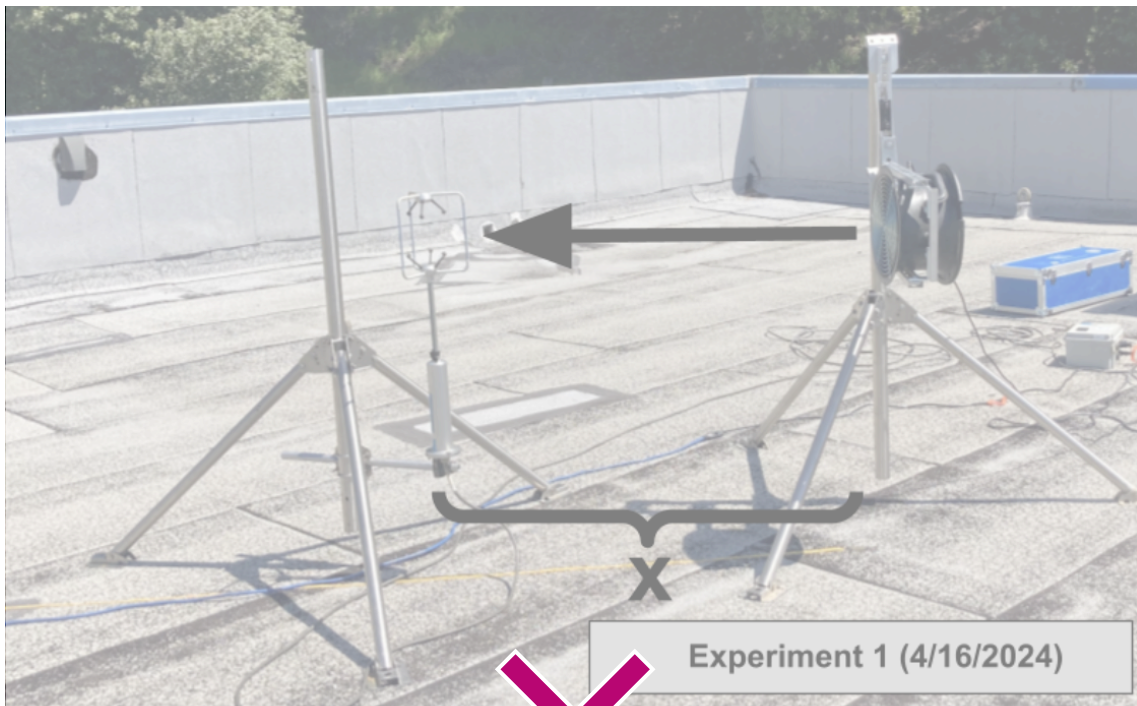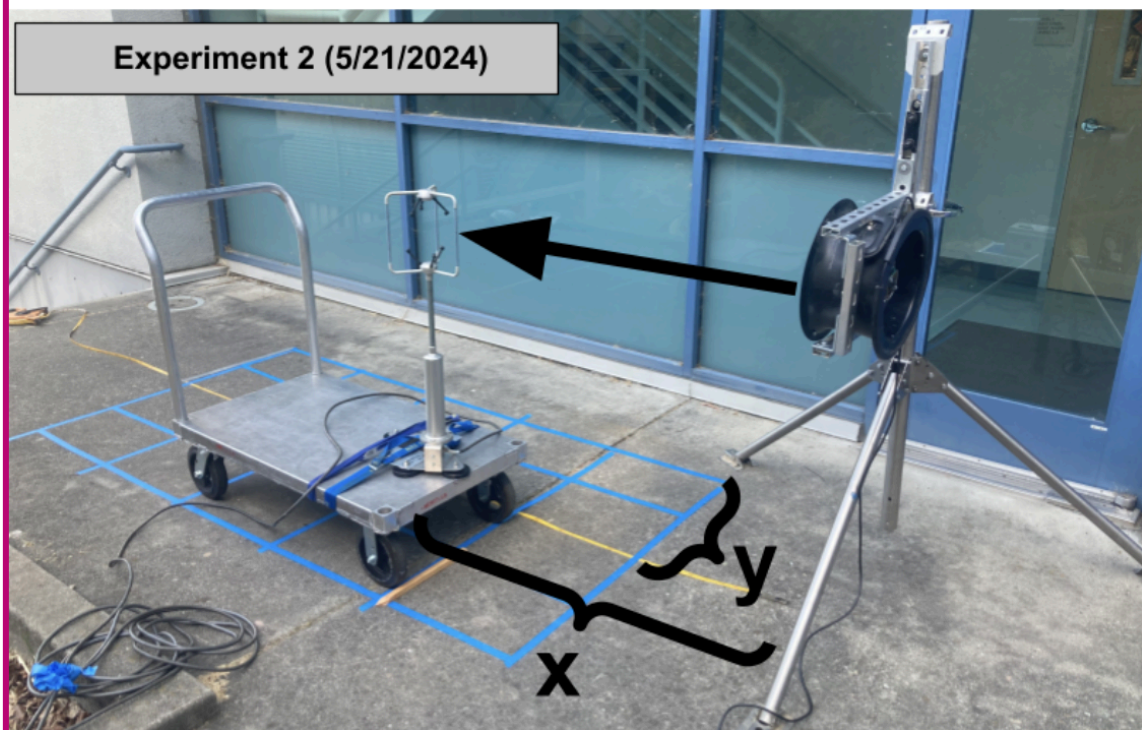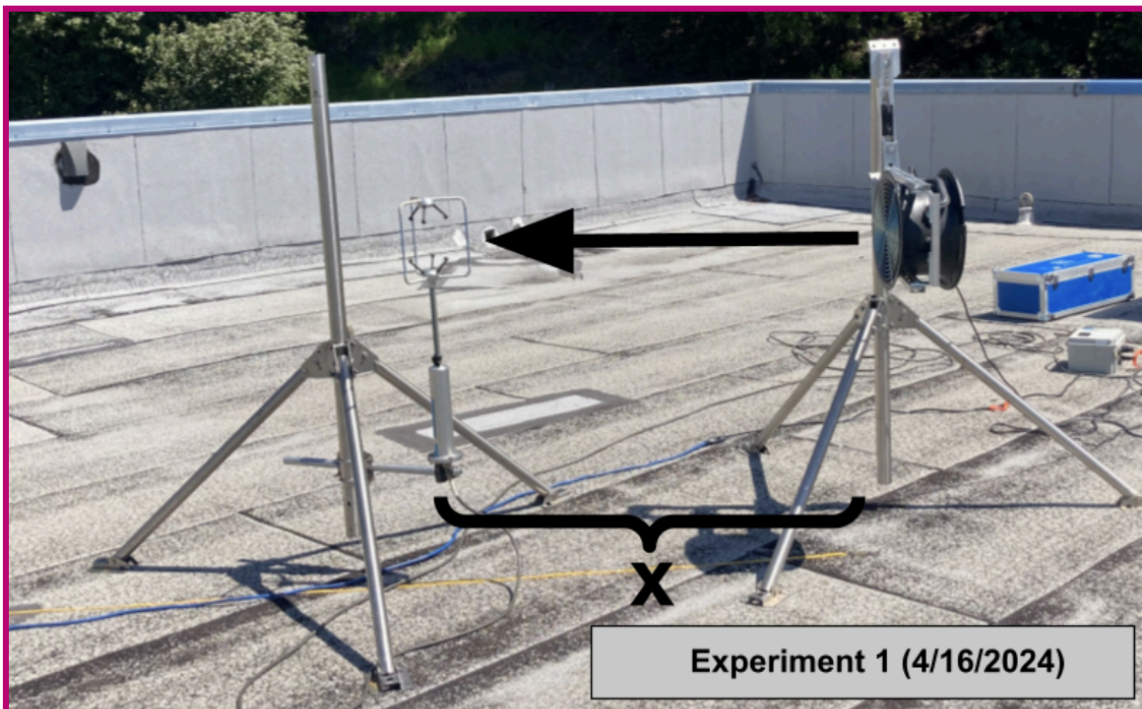
Figure 2: Experimental setup for fan characterization experiments, using an anemometer placed at a downwind distance x and crosswind distance y (second experiment)

2.2 Controlled Release Experiment

To verify and estimate the relevant parameters used in the FAST method, a controlled release experiment was conducted using a range of constant methane leak rates. The SEMTECH HI-FLOW backpack system was used for verification as it has already been validated as a commercial product for estimating leak rates (see Appendix B for more details).

2.2.1 Experimental Setup

The fan position, source position, and sampling position were all 1 meter above ground level, and 1 meter separated from each other along an axis parallel to the ground, with the source placed in between the fan and the sample point (Figure 3). A methane source was prepared by mixing 75 psi of high purity CH_4 with 1425 psi ultra-high purity N2 in a 30 L aluminum cylinder, to obtain a blend of 5.0 ± 0.17%. The source was released from the cylinder at controlled rates using a regulator plumbed through a mass flow controller (Brooks Instrument GF40) programmed with set points corresponding to planned CH_4 emission rates of 1, 2, 5, 10, 20, and 40 g/hr. The sampling for the FAST method was conducted using a Picarro G4302 analyzer [GasScouterTM G4302 Mobile Gas Concentration Analyzer] for measuring the CH_4 concentration and a Gill Windmaster 3-D sonic anemometer placed as physically close together as possible at the sample position (inlet tube mounted within 1 cm of center of anemometer, see Figure 3). The forced advection was done using an MDB fan with no attachments. The fan, anemometer, and data collection systems were powered using a 300 Amp-hour 12V DC battery and inverter, while the Picarro analyzer ran on its internal battery.
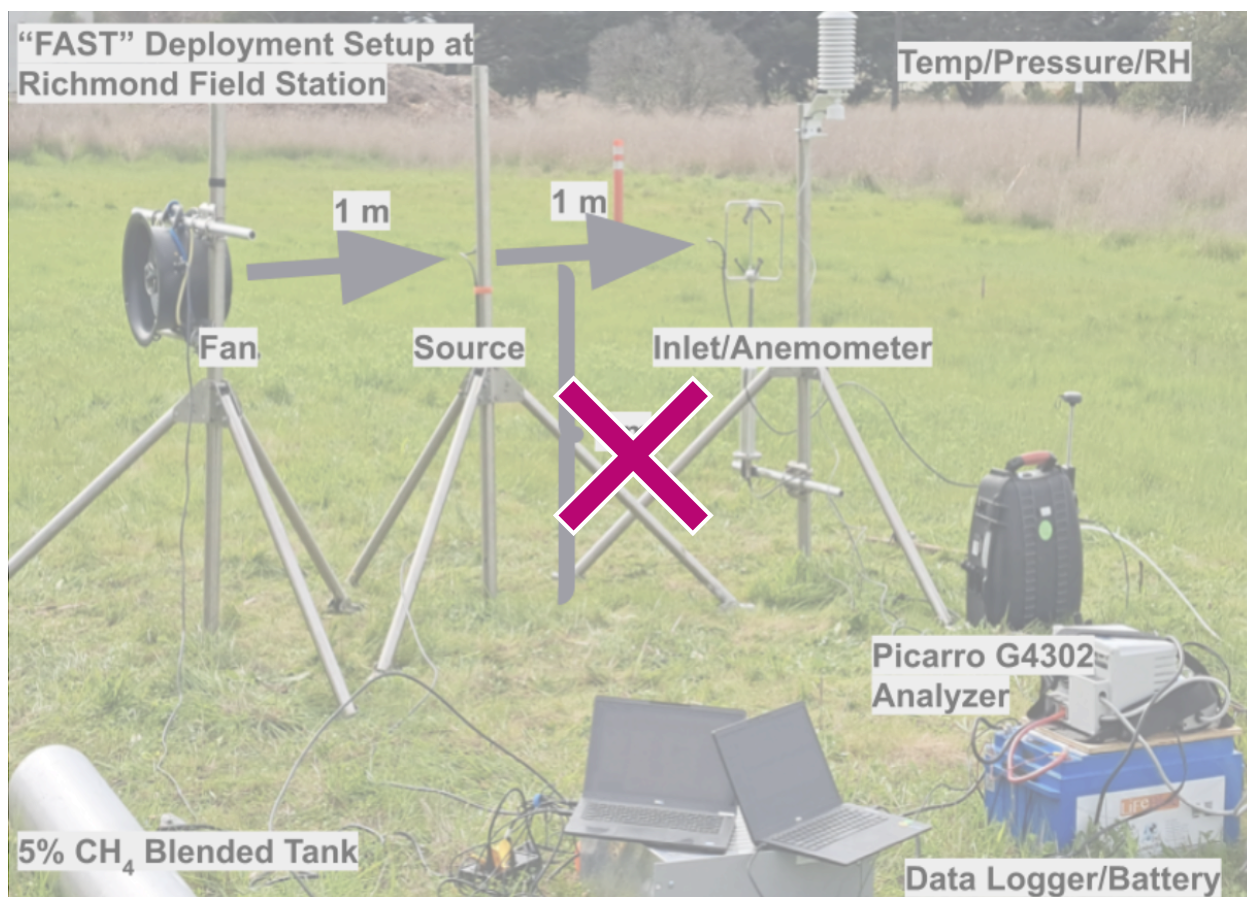
Sensor signals from wind, ambient air temperature, pressure, and source output flow were collected using data loggers, with all data collection system clocks synchronized to within one second of UTC. The experiment began at 18:30 UTC with setup and preparation. At 20:19, the initial experiment for background (1.99 ± 0.36 ppm) measurements started with no source emission. The experiment involved different flow rates with corresponding durations. For each flow rate interval, the SEMTECH measurements were conducted in 2 minutes with no fan, followed by the FAST data collection with 10 minutes without the fan, 10 minutes with the fan at low intensity, and 5 minutes of the fan at high intensity, with 5 to 10 minutes of adjustment between flow rate steps to avoid transient periods. The experiment concluded at 00:21 UTC (the following day).
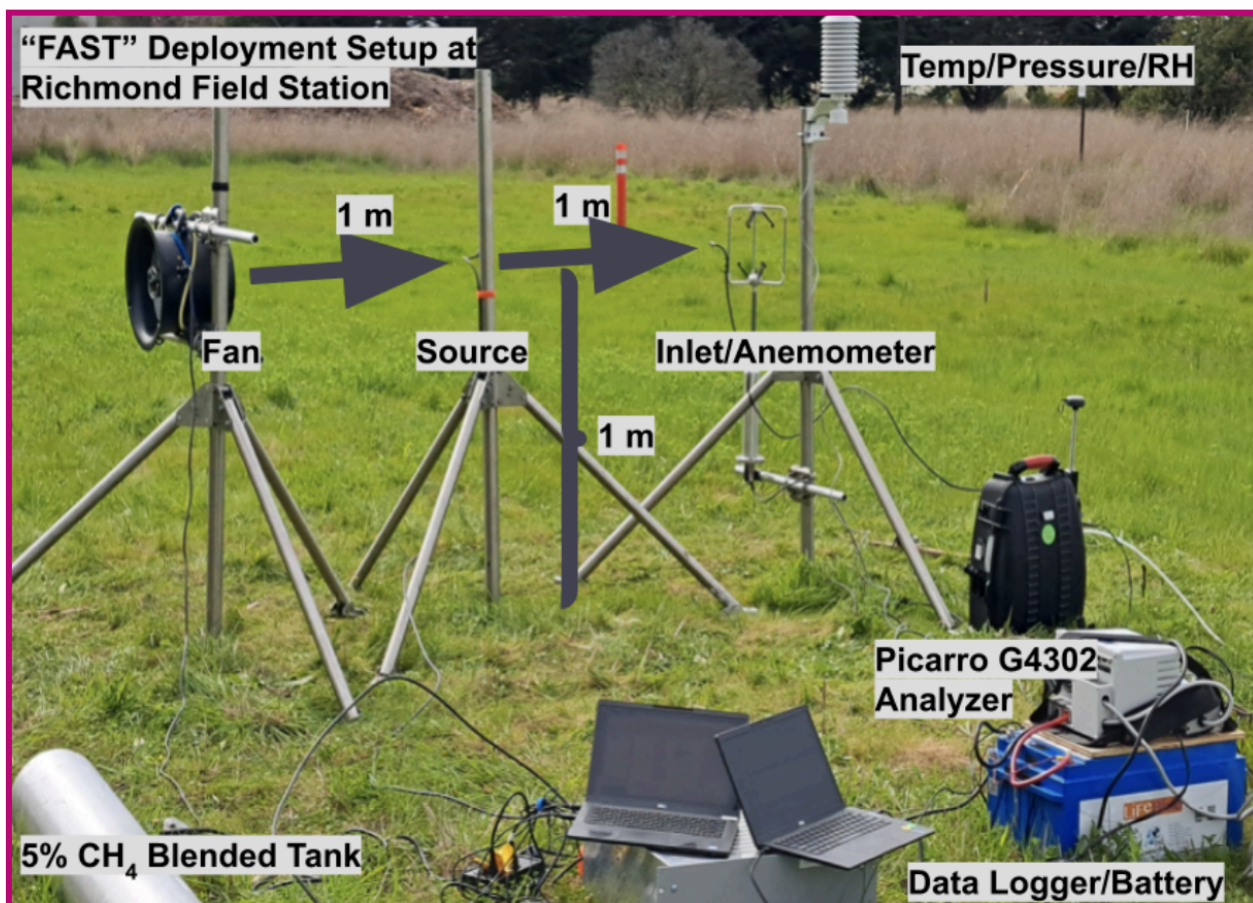
Measured Quantity	Sensor	Measurement Frequency	Data Collection System	Associated System
CH_4 (ppb)	Picarro G4302	2 Hz	Integrated computer	

			running Windows 7	FAST
u, v, w (m/s)	Gill Windmaster 1210-PK-085	10 Hz	Campbell CR1000X Datalogger	
Air Temperature (˚C)	RM Young 41382VC	1 Hz		Controlled Release
Air Pressure (kPa)	Setra 278	1 Hz		
Source Flow (L/min.)	Brooks Instrument GF40	1 Hz	Campbell CR6 Datalogger	

Table 2: Equipment used during the controlled release experiment at Richmond Field Station

"FAST" Deployment Setup at Richmond Field Station

Temp/Pressure/RH

1 m

1 m

Fan

Source

Inlet/Anemometer

Picarro G4302 Analyzer

5% CH$_4$ Blended Tank

Data Logger/Battery

212

12

213

Figure 3: Experimental setup for the controlled release experiment at Richmond Field Station in Richmond, CA. The MDB fan, the inlet for the Picarro G4302 analyzer and the Gill Windmaster 3-D sonic anemometer were mounted at 1 m height at a distance of 2 m from one another (upper limit for the FAST method). A source of 5% methane blended with pure nitrogen was also mounted on a second tripod at a downwind distance of 1 m from the fan and outfitted with a piece of foam to ensure diffuse emissions.

2.2.2 Stoichiometry

The methane source leak rates in g/hr are calculated using measured quantities of source flow, ambient air temperature, pressure, and assumed constant source concentration. The measured quantities reported for each step were averaged over each measurement. The source leak rate Q is described in terms of measured quantities and known constants.

$$Q = C \rho \kappa \qquad (5)$$

where, C is the CH_4 concentration from the source tank at 0.05 ± 0.0017 [mol CH_4 / mol air], ρ is the CH_4 mass density [g/L] at measured ambient temperature and pressure, and

13

228   κ is the corrected output mass flow of the source gas.

229

230 The CH_4 mass density is calculated in terms of measured qualities of ambient air pressure P and temperature T as

231
$$\rho = (M_{CH4}/R)(P/T)$$

232 where, M_{CH4} is molar mass 0.01604 [Kg / mol] of CH_4, and R is the universal gas constant 8.31446 [(L · kPa)/(K · mol)].

233 The corrected output mass flow κ is calculated from the measured flow rate κ_{std} reported at standard temperature T_{std} of 293

234 Kelvin and measured ambient temperature T as

235
$$\kappa = \kappa_{std}(T/T_{std})$$

236

237 Rewriting Q in terms of measured quantities we find:

238
$$Q = \alpha CP\kappa_{std} \tag{6}$$

239 where,

240 $\alpha = [M_{CH4}/(RT_{std})]$

241

242 The source leak rate uncertainty σ_Q (shown as error bars on Q estimates) is estimated from uncertainties in source

243 concentration C, measured quantities of ambient air pressure P and output flow κ_{std}

244 $\sigma_Q = \alpha\sqrt{(P\kappa_{std}\sigma_C)^2 + (C\kappa\sigma_p)^2 + (CP\sigma_\kappa)^2}$ (7)

245 where the uncertainties σ_P and σ_κ are standard deviations of averaged data from the measurement windows. The time series

246 of flow rates and measured atmospheric pressure during the course of the experiment are shown in Figure 4.

247

248 Similarly, the uncertainty in the flow rate estimated by FAST method can be written as:

249
$$\sigma_{\hat{Q}} = \sqrt{\left(K_{FAST}\,\underline{C_{CL}}\,\sigma_{\underline{u_{CL}}}\right)^2 + \left(K_{FAST}\,\underline{u_{CL}}\,\sigma_{\underline{C_{CL}}}\right)^2 + \left(\underline{C_{CL}}\,\underline{u_{CL}}\sigma_{K_{FAST}}\right)^2}$$
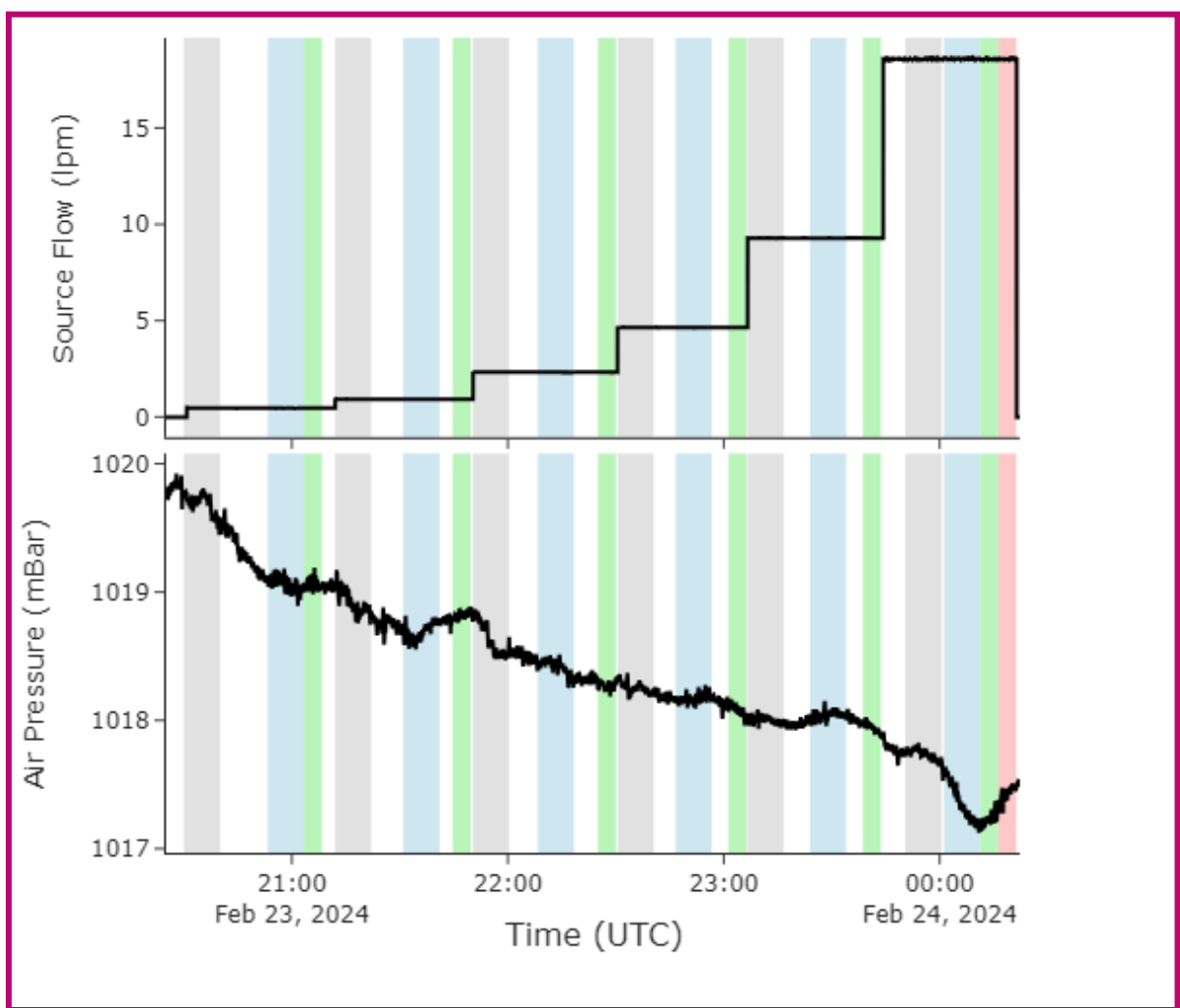
250   (8)

251 where $\sigma_{u_{CL}}$ is the standard deviation of the wind speed in the downwind direction, $\sigma_{C_{CL}}$ is the standard deviation of the

252 concentration measurements and $\sigma_{K_{FAST}}$ is the standard error in the estimate of K_{FAST} as shown in Figure 7 and Table 4.

14

253
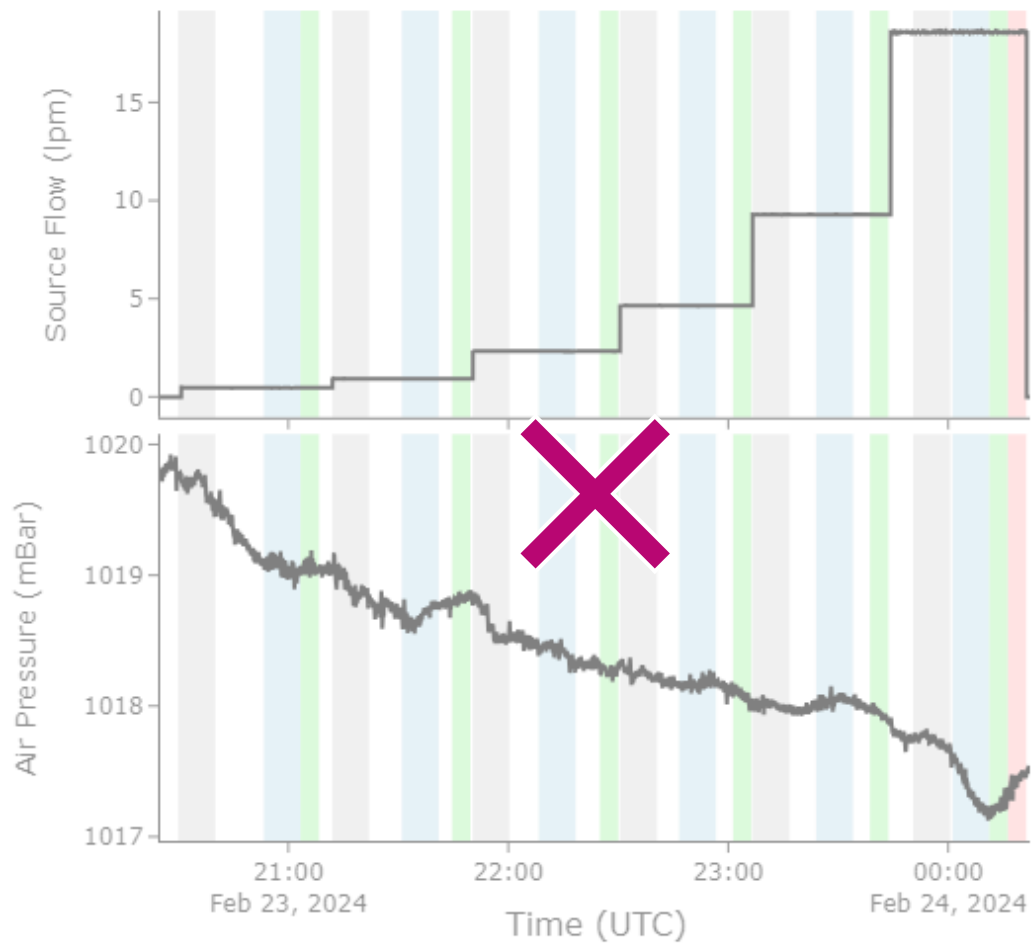
15

Figure 4: Time series of the output flow rate (liters per minute) throughout the Richmond controlled release experiment with shaded areas indicating the set measurement windows: gray for no fan state, blue for fan on at low speed, green for fan on at high speed, and red for maximum fan speed at the end of the experiment.

2.2.3 Data Filtering by Wind Direction

In order to optimize the FAST method under strong crosswind conditions, filtering was applied to improve data quality and estimate emissions more accurately. Despite the advection from the fan, strong crosswind interference introduces variability in both the concentration (C) and wind speed (u) measurements. Filtering addressed this issue by excluding data associated with wind directions unlikely to transport emissions directly to the sensors.

16

265 To filter the data, we first calculate the wind direction (Θ_i) from the x- and y-direction wind components (u and v) within a
266 normalized range of [0, 360) degrees for each data point as follows:

267 $$\Theta_i = ((arctan2(v, u) * \frac{180}{\pi}) + 360) \; mod \; 360 \qquad (9)$$

268 The mean wind direction, Θ_{mean}, is then computed as the arithmetic average of the normalized wind directions:

269 $$\Theta_{mean} = \frac{1}{N} \sum_{i=1}^{N} \Theta_i \qquad (10)$$

270 where N represents the total number of data points in a given measurement period.

271 We then apply a filter angle (ϕ) symmetrically around the mean wind direction to define the range of included data. The
272 lower (Θ_{lower}) and upper (Θ_{upper}) bounds of the filtered range are defined as:

273 $$\Theta_{lower} = (\Theta_{mean} - \frac{360 - \phi}{2}) \; mod \; 360 \qquad (11)$$

274 $$\Theta_{upper} = (\Theta_{mean} + \frac{360 - \phi}{2}) \; mod \; 360 \qquad (12)$$

275 The wind and methane data are then filtered to include only directions within the specified range. If the bounds do not cross
276 the 0 degree/360 degree discontinuity, the filtered data satisfies:

277 $$\Theta_i > \Theta_{lower} \text{ and } \Theta_i < \Theta_{upper} \qquad (13)$$

278 and when the bounds span the discontinuity, data satisfying the following conditions are used:

279 $$\Theta_i > \Theta_{lower} \text{ or } \Theta_i < \Theta_{upper} \qquad (14)$$

280 Figure 5 illustrates the impact of filtering on the time series of wind and methane concentration data, for a 1 g/hr
281 release from the Richmond Field Station experiment (N = 300). As the filter angle decreases, more data from crosswind and
282 background noise is excluded (shown in red) and the mean wind speed (u) and concentration (C) values change, resulting in
283 different estimates from the FAST method. We found that a filter angle of 300° effectively aligns the analysis with wind
284 directions closely aligned with the source when accounting for plume spread within x < 2 m.
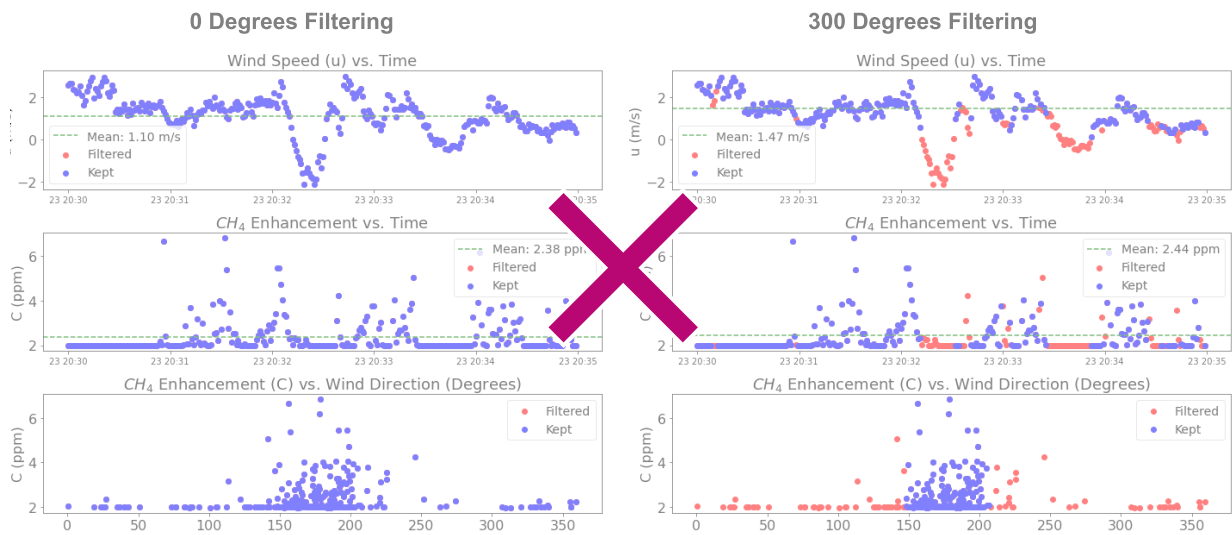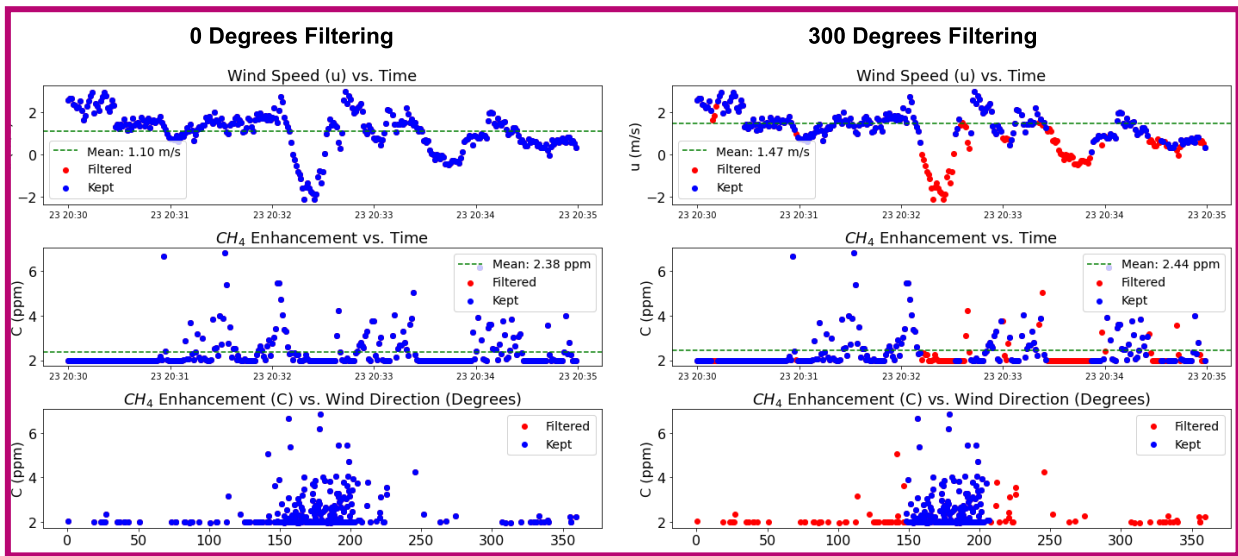
Figure 5: Time series of wind speed (u) and methane enhancement (C) as well as C vs. wind direction (in degrees) for a 'no fan' release of 1 g/hr at the Richmond Field Station. Kept data are shown in blue while filtered data are shown in red. Mean wind speed and concentration over the 5 minute measurement period are shown in green.

2.3 Field Experiments

The FAST method was tested on four wells during two field campaigns, two in Texas (6 and 7 February) and two in Oklahoma (14 March), during the spring of 2024. For all field measurements, a similar setup was used to that in the Richmond Field Station controlled release experiment. During the experiments in Texas, the background wind velocity was < 1 m/s, so only the Low Fan setting was used for the two wells. In Oklahoma, background wind speeds were much higher than those in Richmond, so both the Low Fan and High Fan settings were used. At each well, we measured background

18

297 (upwind) methane concentrations using the Picarro for five minutes and this background value was subtracted from the

298 methane concentrations collected during the FAST method to determine the enhancement. Figure 6 shows images of the four

299 wells discussed in the paper with the FAST method setup. For each well, SEMTECH and FAST measurements were taken;

300 FLIR measurements were taken in Texas only.

301

302
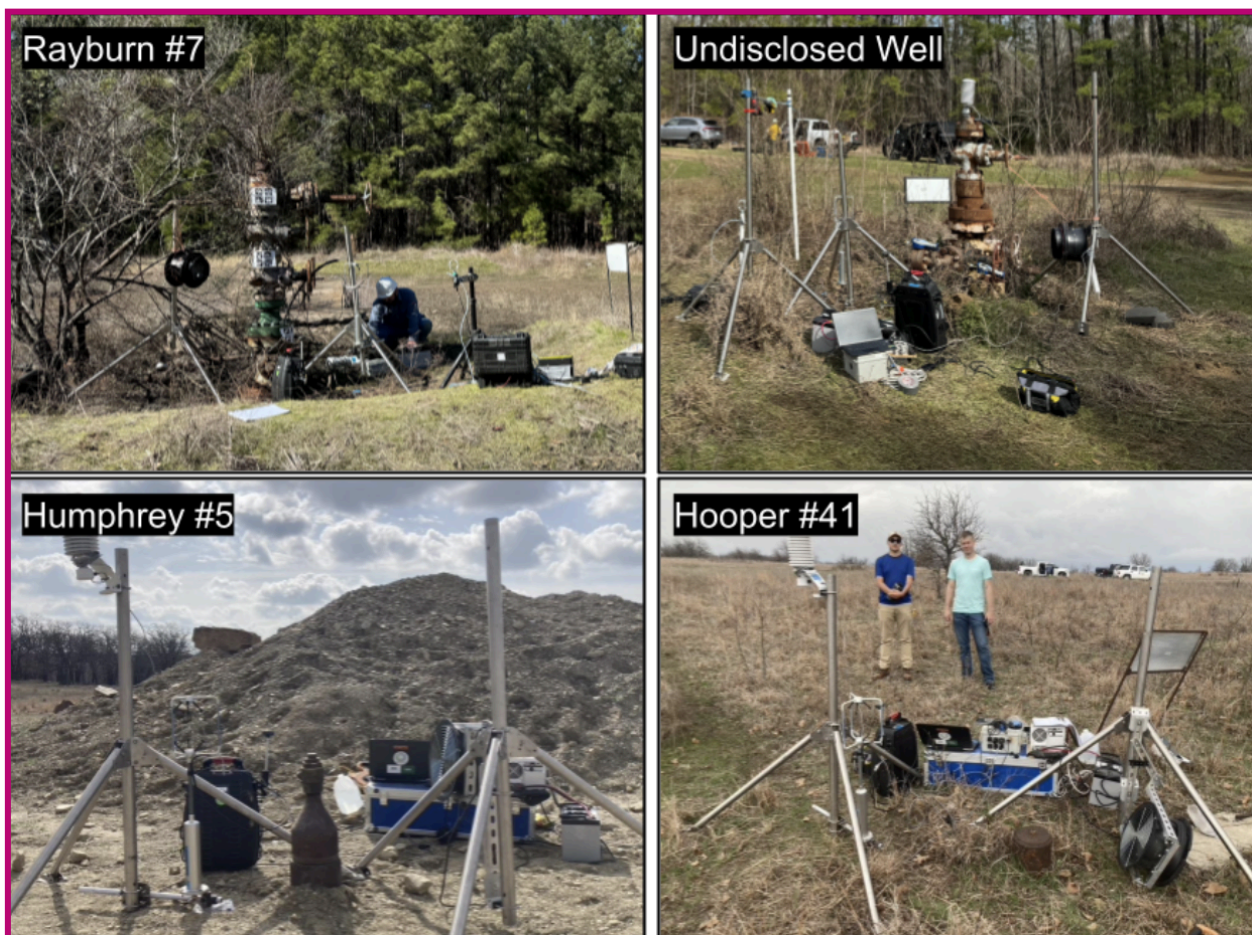
Figure 6: Wells measured in Lufkin, Texas (top) and Barnsdall, Oklahoma (bottom) using the FAST method. Both wells in Texas were of the "christmas tree" variety (multiple potential leak points) and were measured using No Fan and Low Fan speeds because the background wind speeds were < 1 m/s. Both wells in Oklahoma were lower to the ground, had only one leak point and were measured with No Fan, Low Fan and High Fan speeds due to the higher background winds (> 1 m/s).

3 Results

3.1 Fan Characterization Results

     Detailed results of the fan characterization experiments are provided in Appendix C. These experiments demonstrated that the High fan setting produced a more stable and uniform plume under higher background wind conditions, while the Low setting was sufficient for generating a stable plume in the absence of background wind. Wind speed measurements showed that the primary flow velocity decreased with downwind distance, reaching background levels beyond

21

316 approximately 2 meters. Analysis of the standard deviation of wind direction confirmed that plume dispersion followed a
317 square-root dependence on distance for x < 2 meters, in agreement with theoretical expectations. Beyond this range,
318 crosswind turbulence caused significant deviations from the expected dispersion behavior, leading to increased variability
319 and instability in the plume structure. Additionally, measurements taken off the plume centerline (y ≠ 0) exhibited greater
320 variability due to crosswind effects, reinforcing the importance of positioning sensors along the centerline (y = 0) to ensure
321 consistent and reproducible measurements. Based on these findings, all field experiments were conducted with sensors
322 placed within 2 meters of the fan and along the centerline.
323
324   Furthermore, based on our fan experiments, we were able to estimate the parameters needed to calculate K_{FAST} using
325 Equation 4. We measured the blade length of the MDB fan (l_{fan}) and estimated the turbulence intensity i_{fan} as the mean of
326 the turbulence intensity measured in the first fan experiment during the High and Low fan settings for x < 2m (see Figures
327 C1 and C2). Using these values ($\beta = 1$, $i_{fan} = 0.23$, $l_{fan} = 0.13\ m$, $x_0 = 2\ m$), the effective K_{FAST} would be

328 $K_{FAST} = \pi \beta\, i_{fan}\, l_{fan}\, x_0 = 0.19\ m^2$, which matches the value determined during the controlled release experiment
329 with maximum filtering (300 degrees).
330
331 **3.2 Experimental Determination of K_{FAST}**
332
333   Results from the Richmond Field Station controlled release experiment are summarized in Table 3. Using Equations
334 7 and 8, an estimate of the actual source rate (Q) was obtained which nearly matched the intended target rates of 1, 2, 5, 10,
335 20 and 40 g/hr. The SEMTECH HI-FLOW performed very well during the controlled release study, almost matching the
336 exact values derived from stoichiometry. The FAST method estimates (generated using 10 minute averages and $K_{FAST} = 0.19$
337 m^2) also match the source rate quite well, however with much larger uncertainties than the SEMTECH. Without the fan (No
338 Fan), the FAST method tends to overestimate the lower range (1-5 g/hr) and severely underestimate the upper range (10-40
339 g/hr). This is greatly improved via the use of the fan, with the Low Fan setting performing slightly better in the upper range
340 and the High Fan setting performing better in the lower range. These discrepancies could also be due to fluctuations in the
341 background wind throughout the experiment which may have biased the results.
342

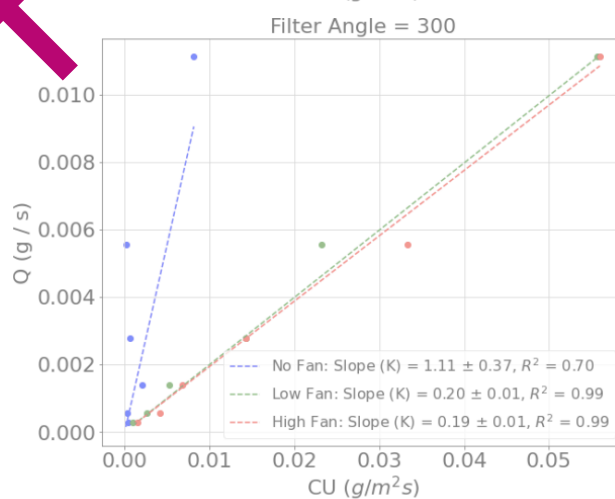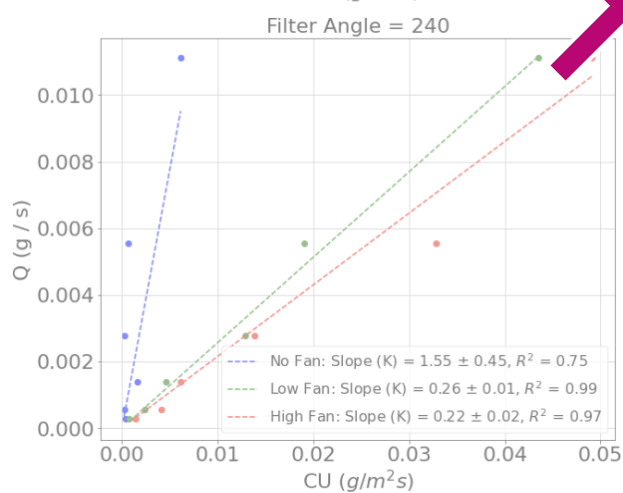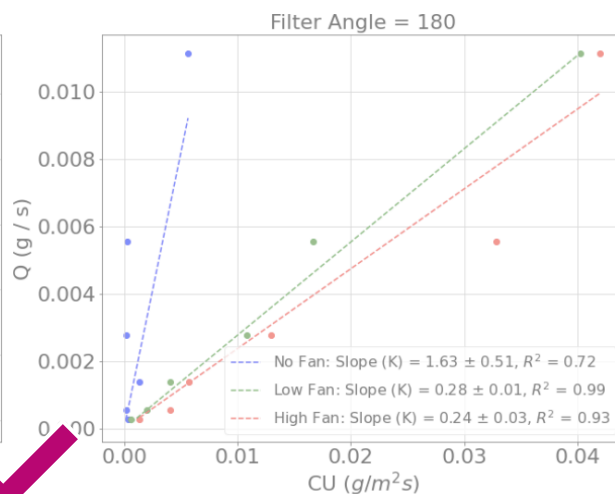| Source Rate $Q \pm \sigma_Q$ (g/hr CH_4)	SEMTECH (g/hr CH_4)	FAST (No Fan) (g/hr CH_4)	FAST (Low Fan) (g/hr CH_4)	FAST (High Fan) (g/hr CH_4)
0.93 ± 0.03	0.96 ± 0.03	0.27 ± 2.94	0.65 ± 0.51	1.01 ± 0.50
1.86 ± 0.06	1.89 ± 0.05	1.34 ± 3.81	1.85 ± 1.17	2.81 ± 0.78
4.66 ± 0.17	4.62 ± 0.08	8.23 ± 16.14	3.65 ± 2.50	4.65 ± 2.38
9.33 ± 0.32	9.25 ± 0.16	2.40 ± 11.62	10.29 ± 4.99	9.75 ± 4.08
18.67 ± 0.63	18.30 ± 0.33	0.52 ± 2.01	16.74 ± 9.70	22.80 ± 7.14

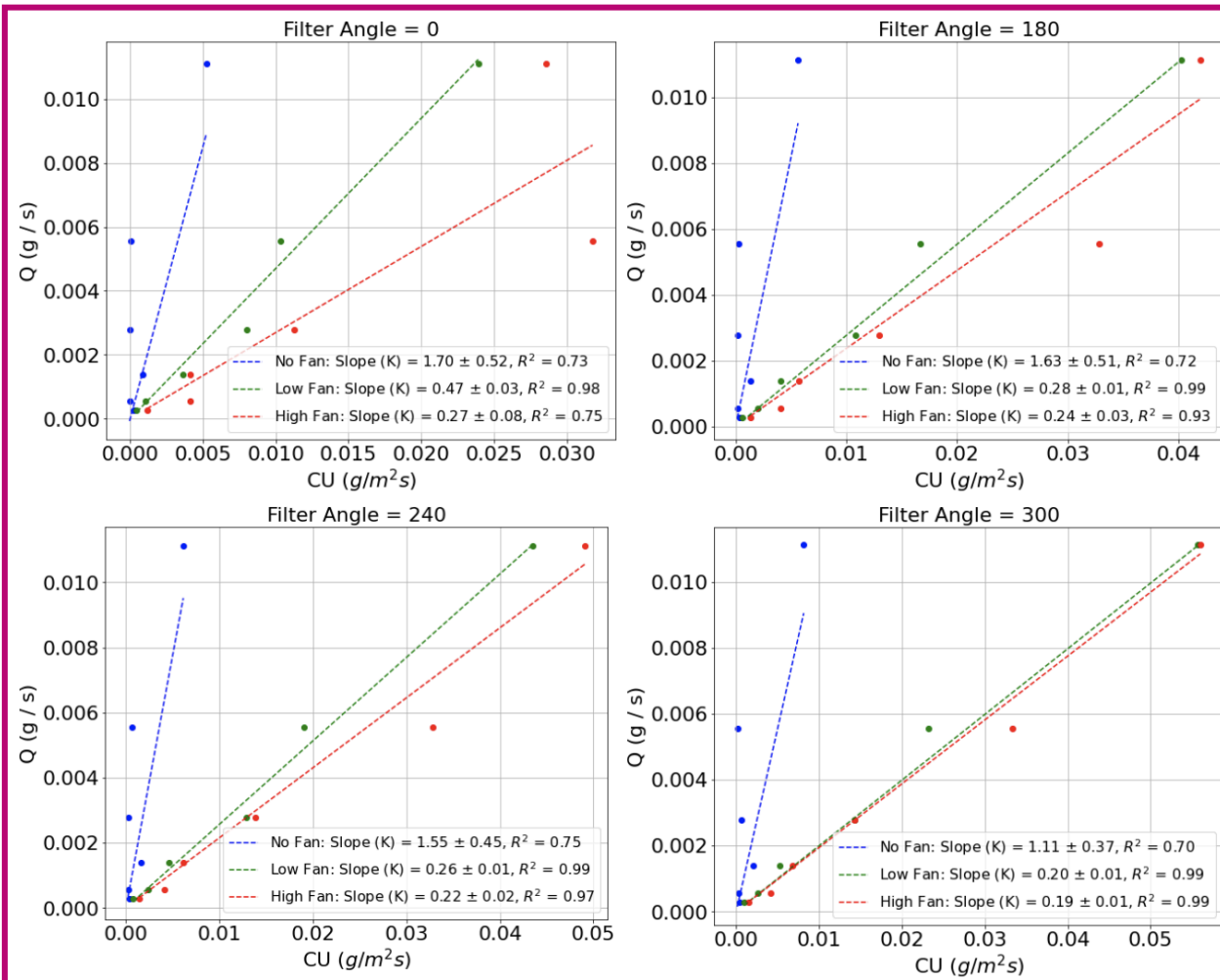|				
37.32 ± 1.27	36.90 ± 0.53	32.54 ± 75.92	40.13 ± 21.70	38.20 ± 17.40

Table 3: Comparison of the desired (target) and true (stoichiometric) release rate with those measured by the SEMTECH and FAST method (with 300 degrees of filtering) during the controlled release experiment at Richmond Field Station.

Filter Angle = 0

No Fan: Slope (K) = 1.70 ± 0.52, R^2 = 0.73
Low Fan: Slope (K) = 0.47 ± 0.03, R^2 = 0.98
High Fan: Slope (K) = 0.27 ± 0.08, R^2 = 0.75

Filter Angle = 180

No Fan: Slope (K) = 1.63 ± 0.51, R^2 = 0.72
Low Fan: Slope (K) = 0.28 ± 0.01, R^2 = 0.99
High Fan: Slope (K) = 0.24 ± 0.03, R^2 = 0.93

Filter Angle = 240

No Fan: Slope (K) = 1.55 ± 0.45, R^2 = 0.75
Low Fan: Slope (K) = 0.26 ± 0.01, R^2 = 0.99
High Fan: Slope (K) = 0.22 ± 0.02, R^2 = 0.97

Filter Angle = 300

No Fan: Slope (K) = 1.11 ± 0.37, R^2 = 0.70
Low Fan: Slope (K) = 0.20 ± 0.01, R^2 = 0.99
High Fan: Slope (K) = 0.19 ± 0.01, R^2 = 0.99

352
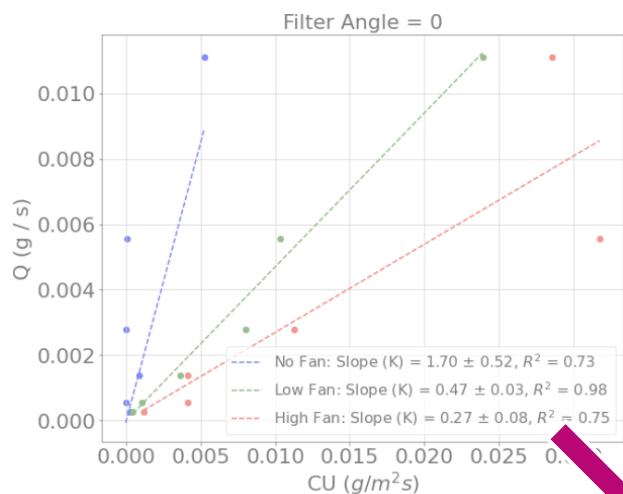
24

Figure 7: Measured mean C * U (along x) vs. known Q (along y) for the control release experiment used to determine the values of K_{FAST} (slopes) for a range of fan speeds and filtering angles.

By using the known values of Q from stoichiometry (source rate) and the measured values of C and u during the controlled release experiment, the experimentally determined values of K_{FAST} for different filter angles and fan speeds are estimated via Equation 3. By inverting Equation 3 to solve for K_{FAST}, $K_{FAST} = \dfrac{\overline{C_{CL}}\,\overline{u_{CL}}}{Q}$ where the known value of Q and 10 minute averages of C_{CL} and u_{CL} are used to estimate K_{FAST}. The resulting values for K_{FAST} are shown as the slopes of the lines in Figure 7 along with the uncertainties resulting from standard error estimates on the linear regression used to generate the line of best fit. As expected, the No Fan scenario has a much higher value of K_{FAST} with higher overall uncertainty due to the variation of the natural wind direction and speed. Without filtering the data by wind direction, the K_{FAST} values are larger (likely due to more dispersion from crosswinds). Furthermore, K_{FAST} values at the low and high fan speeds do not agree, although K_{FAST} is theoretically independent of fan speed (per Equation 4). As more and more crosswind is filtered (Filter Angle approaches 360 degrees), the low and high fan speeds converge to a K_{FAST} of around 0.19 m², as expected. All fits are done with a 0 intercept and standard errors are used to estimate the uncertainty of K_{FAST}. Table 4 shows the resulting

25

experimentally determined values of K_{FAST} and their corresponding uncertainties which were used to estimate emissions and corresponding uncertainties from field measurements.

Filter Angle	No Fan	Low Fan	High Fan
0 Degrees	1.70 ± 0.52	0.47 ± 0.03	0.27 ± 0.08
180 Degrees	1.63 ± 0.51	0.28 ± 0.01	0.24 ± 0.03
300 Degrees	1.11 ± 0.37	0.20 ± 0.01	0.19 ± 0.01

Table 4: Values of K_{FAST} in m^2 and their associated uncertainties under various filter and fan conditions determined from the Richmond controlled release experiment.

3.3 Field Campaigns

3.3.1 Texas Field Campaign

The first field campaign that measured orphaned wells using the FAST method took place in February 2024 in collaboration with multiple agencies. The U.S. Forest Service (USFS) invited the U.S. Department of Energy's Consortium Advancing Technology for Assessment of Lost Oil and Gas Wells (CATALOG) team to help measure and assess emissions from certain wells being plugged using funds from the Infrastructure Investment and Jobs Act (IIJA). The FAST method was deployed in the field campaign to understand emission patterns better and help allocate sealing funds more efficiently.

Rayburn #7

Rayburn #7 is an oil production well identified by API number 4200530245 and associated with district/lease number 06/13688. Its geographical coordinates are 31.0865, -94.1974, and its total depth is 12,927 feet. On February 6, 2024 during the initial detection of Rayburn #7, a small leak was found from a threaded port on a valve junction 1.2 meters above the ground by sniffing the casing of the well with the Picarro G4302. The well is situated in a large clearing with a gravel pad and other infrastructure, surrounded by an embankment. A plastic spill tub and several 500-gallon drums were observed close to the wellhead. Furthermore, a compressor station and separation/storage infrastructure are located in the corner of the clearing. No leak was detected on any of the other infrastructure in the area. A Gill R3-50 sonic anemometer was placed at the height of 1.2 meters and 0.94 meters away from the methane source, alongside with the inlet to the Picarro G4302 methane detector. Sampling commenced at 12:20 under ambient conditions for 60 minutes. The background methane concentration was 2.11 ppm. Following this, there were two more sets of sampling periods: 30 minutes each for ambient conditions and low fan conditions. The SEMTECH measured an emission rate of 2.86 grams per hour, with a standard deviation during the averaging period of ± 0.04g/h (Figure B2a). The FLIR camera could not provide a clear visual indication of the leak.
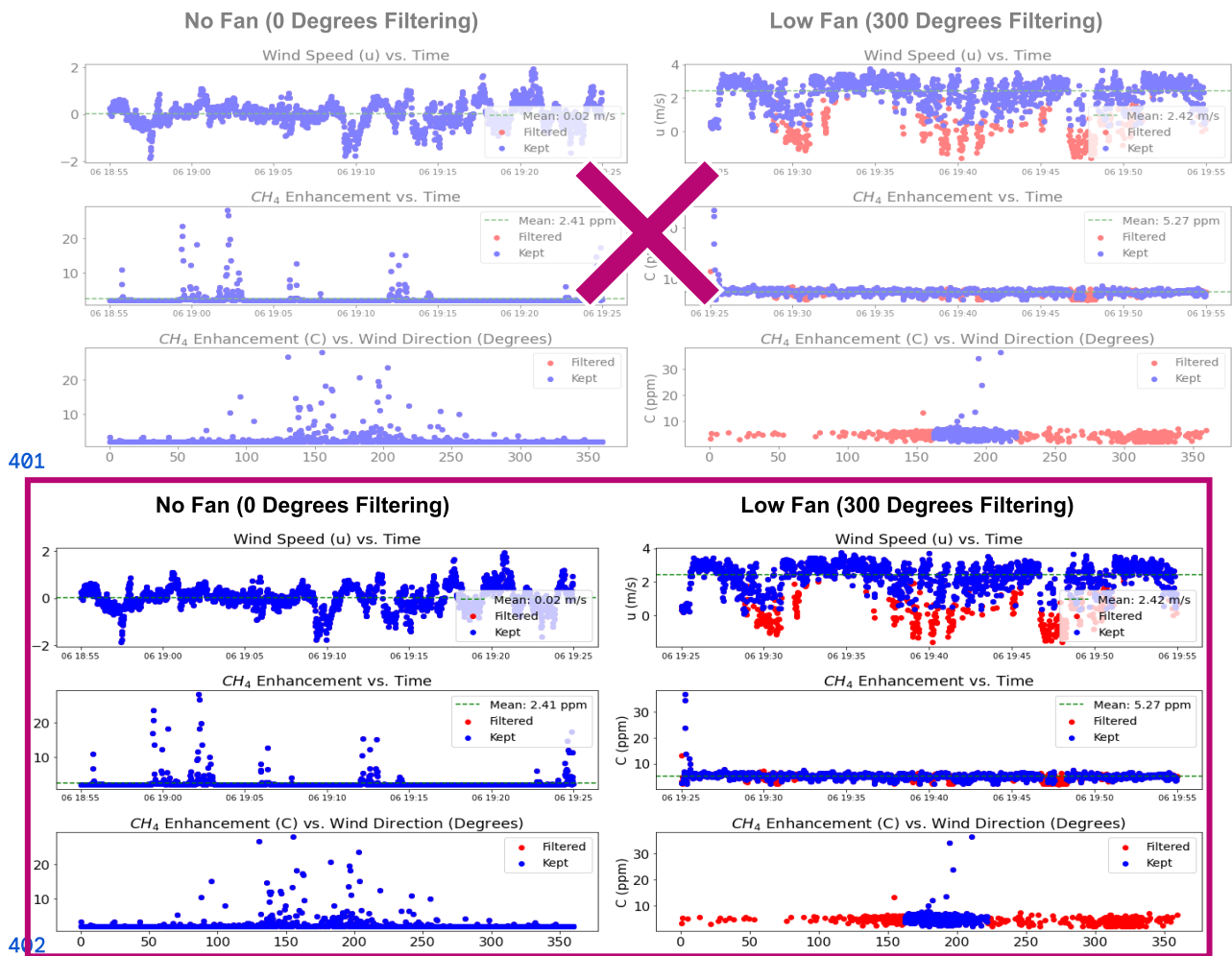
Figure 8: Time series of wind speed (u) and methane enhancement (C) as well as C vs. wind direction (in degrees) for 'no fan' setting from a 'low fan' setting. Kept data are shown in blue while filtered data are shown in red. Mean wind speed and concentration over the 30 minute measurement periods are shown in green.

Figure 8 illustrates the effect of using the fan on the time series of concentration and wind speed measurements at Rayburn #7, providing insight into the variability of methane concentrations and plume enhancements. Without the fan (Figure 8, left), the average wind speed in the x-direction (u) over the 30-minute measuring period was approximately 0 m/s. However, infrequent gusts in the x-direction caused spikes in methane concentrations, ranging from about 10 to 20 ppm above background levels. These spikes were spread across a wide range of directions, between 100 and 250 degrees, indicating variable plume dispersion under stagnant conditions. With the fan on at a low setting (Figure 8, right), the mean wind speed in the x-direction (u) increased to approximately 2 m/s, and the plume became more stable. The methane concentration spikes were more concentrated in direction, between 180 and 210 degrees, corresponding to the airflow from the fan. While a large spike was observed at the start of the low fan measurement, likely due to the fan turning on, the concentration stabilized to around 5 ppm above background levels after this initial adjustment.

Undisclosed Well

The methane emission detection and monitoring experiment at this undisclosed location identified two leak points on one wellhead. The FLIR did not detect any emissions from either of the leak sources. There was a small leak at the end of a main pipe flange and a more significant leak in a connection thread on the same flange, which was the primary point source. The FAST system was set up at 11:45 UTC on February 7, 2024, pointed at 315 degrees N, with the fan turned off. The fan was located 58 cm above the ground and 87 cm upwind from the source, which is within the range of <1 m. The Gill R3-50 sonic anemometer and Picarro G4302 gas analyzer inlets were positioned 73 and 71 cm above the ground and 97 and 95 cm horizontally from the source, respectively. The primary source was at a height of 47 cm. The background methane concentration was 2.08 ppm. The experiment with the fan turned on started at 13:22 UTC. Data was collected for two 15-minute periods with the fan on and two 15-minute periods with the fan off. Analogous to the Rayburn #7 experiment, the anemometer orientation was set in a manner that 0 degrees represents the direction where it is facing the upwind source and fan line. For this experiment, wind direction had favorable conditions, which led to significant data acquisition for the periods without the fan. The SEMTECH measured an emission rate of 0.95 grams per hour, with a standard deviation during the averaging period of ± 0.25 g/h (Figure B2b).

3.3.2. Oklahoma Field Campaign

Humphrey #5

Humphrey #5 is an orphaned well that was located by our team during surveying on March 14th, 2024. The FAST method was set up and measured for 10 minutes at each fan speed (No, Low, High) as shown in Figure 9. The leak was from the top cap of the well head at a height of 0.62 m, and the sensors were positioned downwind at 0.4 m from the leak and a height of 0.65 m. The fan was set up at a height of 0.6 m and an angle of 5 degrees upward (to generate a plume that passed through the anemometer) at 0.5 m upwind of the well. The SEMTECH measured an emission rate of 2.03 grams per hour, with a standard deviation during the averaging period of ± 0.04 g/h (Figure B2c).

444
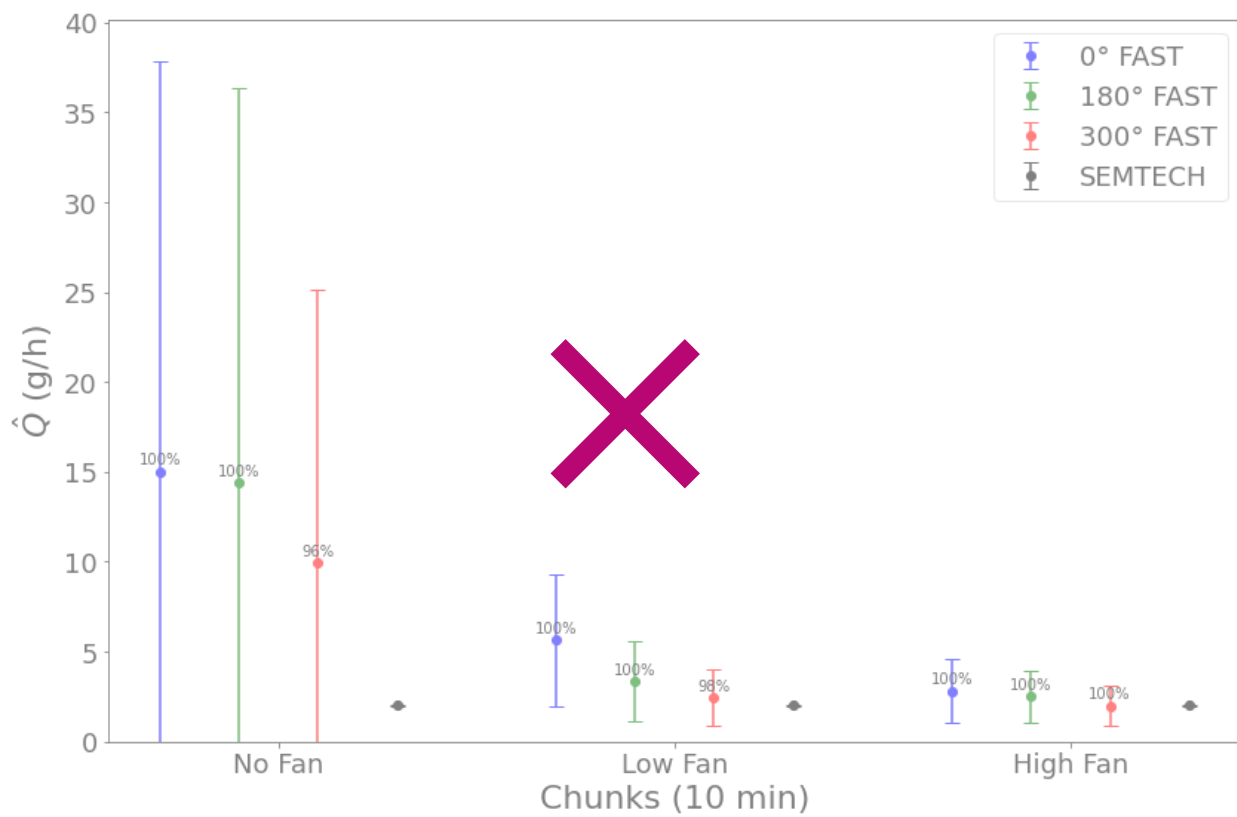
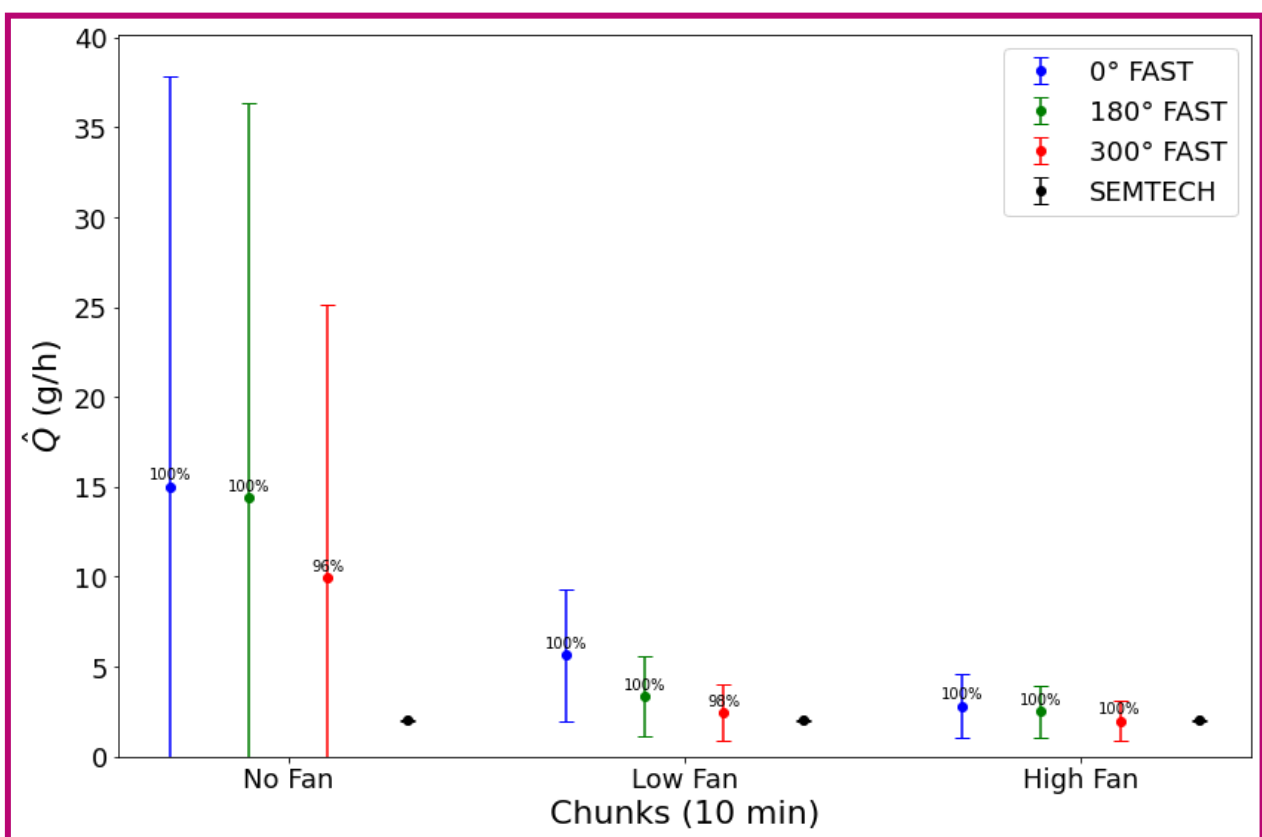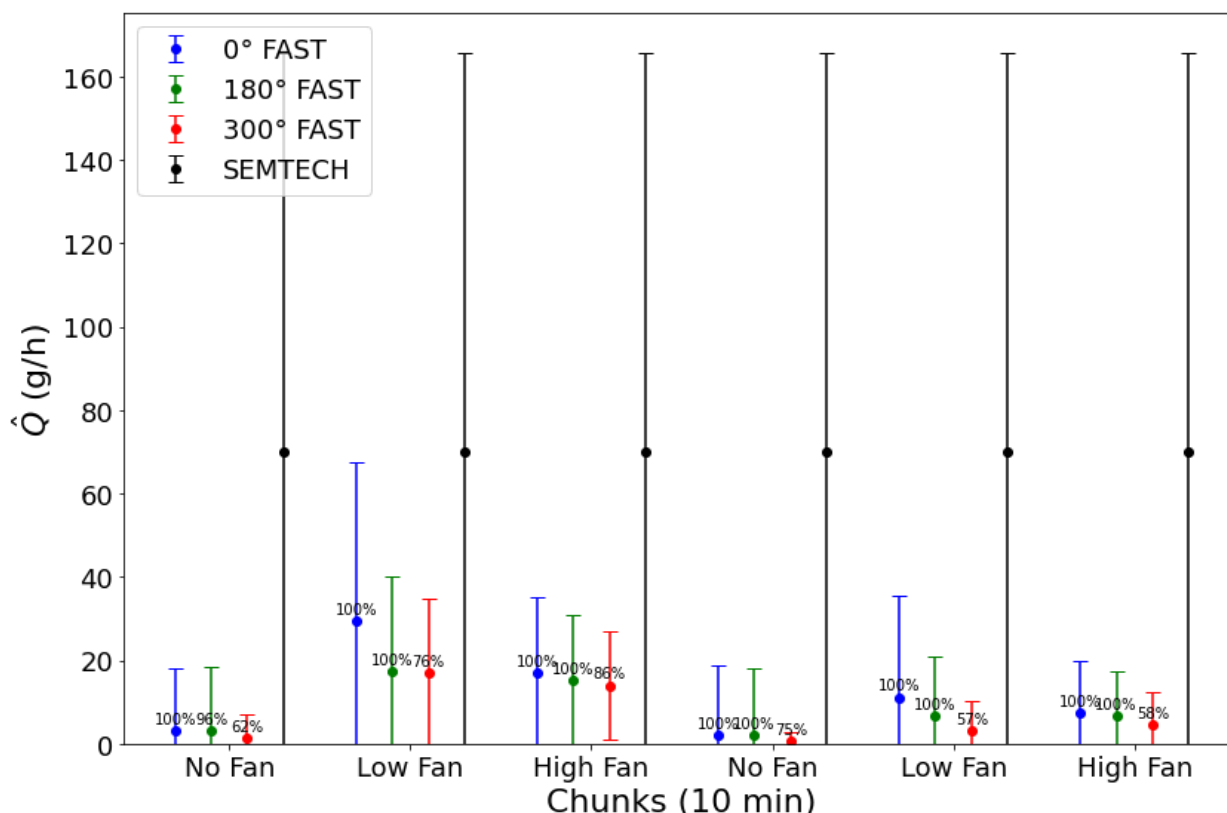**Figure 9**: Estimated leak rates ($\hat{Q}$) and uncertainties ($\sigma_{\hat{Q}}$) from FAST method measured in 10 minute increments (colored) and SEMTECH (black) for Humphrey #5, labeled by percentage of data kept after filtering. For the "No Fan" setting (left most), the estimate is very uncertain and much higher than the SEMTECH.

Hooper #41

      Hooper #41 is another UOW that was also discovered by the team on March 14th, 2024 near Barnsdall, OK. The leak was from the top cap of the well head at a height of 0.25 m, the sensors were positioned downwind at 0.88 m from the leak and a height of 0.65 m. The fan was set up at a height of 0.27 m and an angle of 24 degrees upward at 0.4 m upwind of the well. Interestingly, this well seemed to have a variable leak rate, resulting in a very high uncertainty on the SEMTECH. The SEMTECH measured an intermittent averaged emission rate of 70.14 g/h, with a large standard deviation during the averaging period of ± 95.47 g/h (Figure B2d). The FAST method was used in 10 minute intervals for No, Low, and High fan settings. Due to the highly variable nature of the well, these measurements were repeated in the same intervals for comparison (Figure 10). During both measurement periods, the FAST method estimates the well to only emit around 10 +/- 10 g/h as opposed to 70 +/- 90, which the SEMTECH reported.

Figure 10: Estimated leak rates ($\hat{Q}$) and uncertainties ($\sigma_{\hat{Q}}$) from FAST method measured in 10 minute increments (colored) and SEMTECH (black) for Hooper #41, labeled by percentage of data kept after filtering. Due to the high variability of the well, it was measured twice with the FAST method at 10 minute increments (sequentially). Here, the SEMTECH did not get a good reading due to the instability in the CH_4 concentration of the sampling volume.

The results for Hooper #41 highlight challenges in measuring methane emissions from variable wells and suggest potential limitations in the FAST method. The variable leak rate led to significant uncertainty in SEMTECH readings (± 95.47 g/h), while the FAST method provided more stable estimates (10 ± 10 g/h). However, the fan setup likely failed to fully entrain the emitted gas into the airflow directed toward the sensor, potentially leading to an underestimation of emissions, as supported by SEMTECH data and Figure 10. This limitation is particularly critical for wells with low-height emissions, such as Hooper #41. ~~Despite this, the FAST method shows promise for measuring variable emissions more consistently than SEMTECH.~~ Future work could address this limitation through controlled release experiments at different heights to optimize the fan and sensor configurations for capturing low-lying plumes.

4. Discussion

The results of the field campaigns are summarized in Table 5 and Figure 11. For each of the four wells measured, the FAST method results are based on 10 minute averages and K_{FAST} values corresponding to the fan speed and various levels

31

481 of filtering (0, 180 and 300 degrees) as shown in Figure 7 and Table 4. The uncertainty in the FAST estimates is calculated
482 using Equation 8. Overall, the FAST method agrees with the SEMTECH for both the Low and High fan settings but not for
483 the No Fan settings. These uncertainties decrease with a larger filtering angle and a higher fan speed. Furthermore, emission
484 rate estimates for all four wells were calculated using a Gaussian Plume Model (GPM) and described in Appendix A for
485 comparison.
486

487
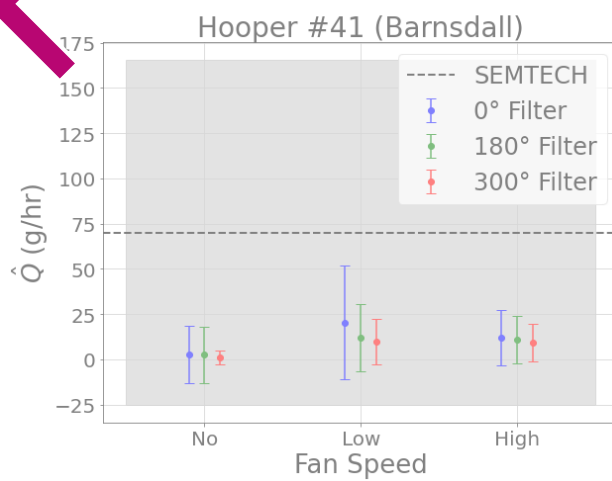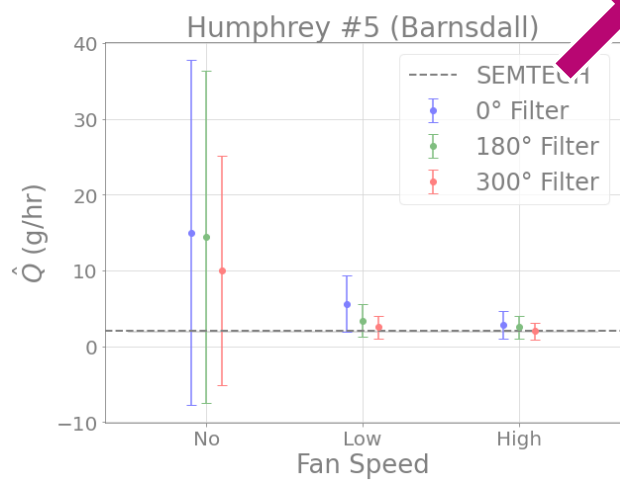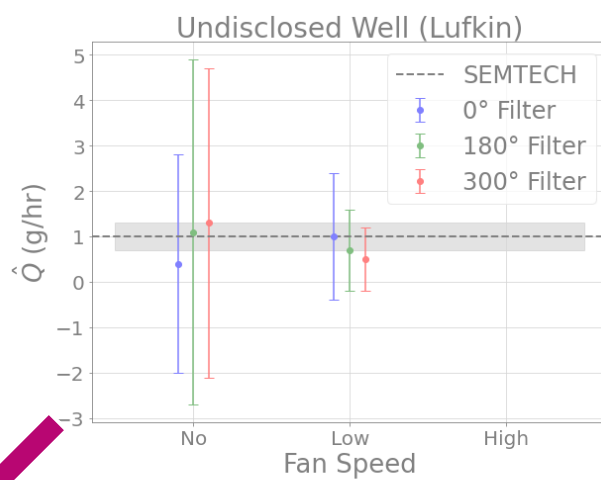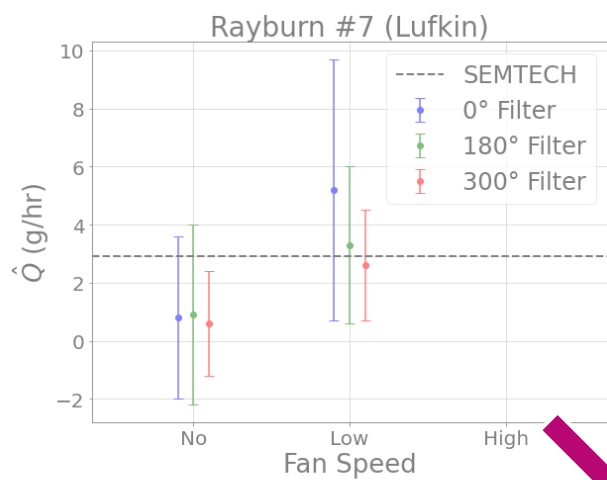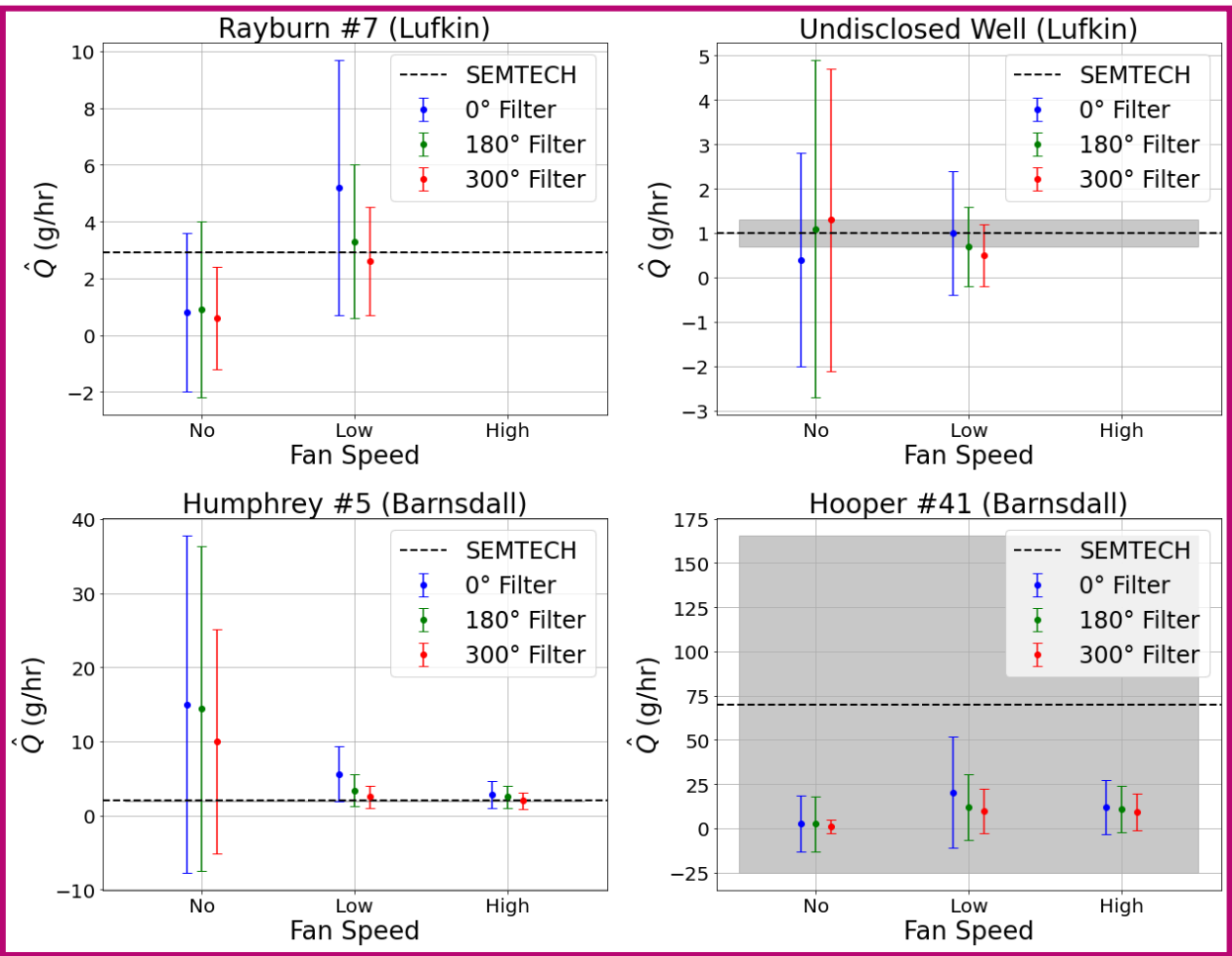
Figure 11: Estimated leak rates ($\hat{Q}$) and uncertainties ($\sigma_{\hat{Q}}$) for the four wells shown in Figure 6 from the SEMTECH (black and gray) and FAST method (colored). SEMTECH is able to get very accurate readings for all wells except Hooper #41 which was a highly variable well.

Date	Well ID	SEMTECH (g/hr)	FAST (0 Filter) (g/hr)	FAST (180 Filter) (g/hr)	FAST (300 Filter) (g/hr)
2024-02-06	Rayburn #7 (Lufkin)	2.9 ± 0.0	Low: 5.2 ± 4.5 No: 0.8 ± 2.8	Low: 3.3 ± 2.7 No: 0.9 ± 3.1	Low: 2.6 ± 1.9 No: 0.6 ± 1.8

2024-02-07	Undisclosed Well (Lufkin)	1.0 ± 0.3	Low: 1.0 ± 1.4 No: 0.4 ± 2.4	Low: 0.7 ± 0.9 No: 1.1 ± 3.8	Low: 0.5 ± 0.7 No: 1.3 ± 3.4
2024-03-14	Humphrey #5 (Barnsdall)	2.0 ± 0.04	High: 2.8 ± 1.8 Low: 5.6 ± 3.7 No: 15.0 ± 22.8	High: 2.5 ± 1.5 Low: 3.4 ± 2.2 No: 14.4 ± 21.9	High: 2.0 ± 1.1 Low: 2.5 ± 1.5 No: 10.0 ± 15.1
2024-03-14	Hooper #41 (Barnsdall)	70.1 ± 95.5	High: 12.1 ± 15.3 Low: 20.2 ± 31.4 No: 2.6 ± 15.8	High: 10.8 ± 13.3 Low: 12.0 ± 18.6 No: 2.6 ± 15.6	High: 9.3 ± 10.4 Low: 9.9 ± 12.7 No: 1.0 ± 4.0

Table 5: Estimated leak rates ($\hat{Q}$) and uncertainties ($\sigma_{\hat{Q}}$) for the four wells shown in Figure 6 from the SEMTECH and FAST method. SEMTECH is able to get very accurate readings for all wells except Hooper #41 which was a highly variable well.

497

498
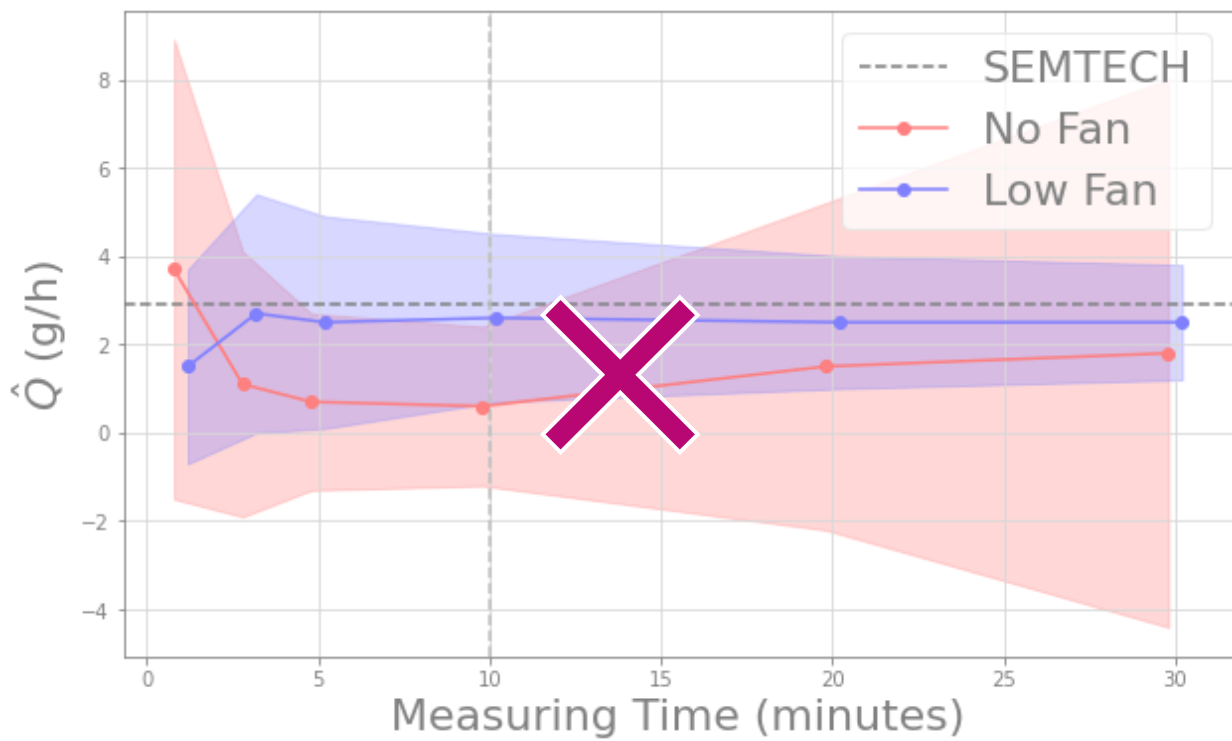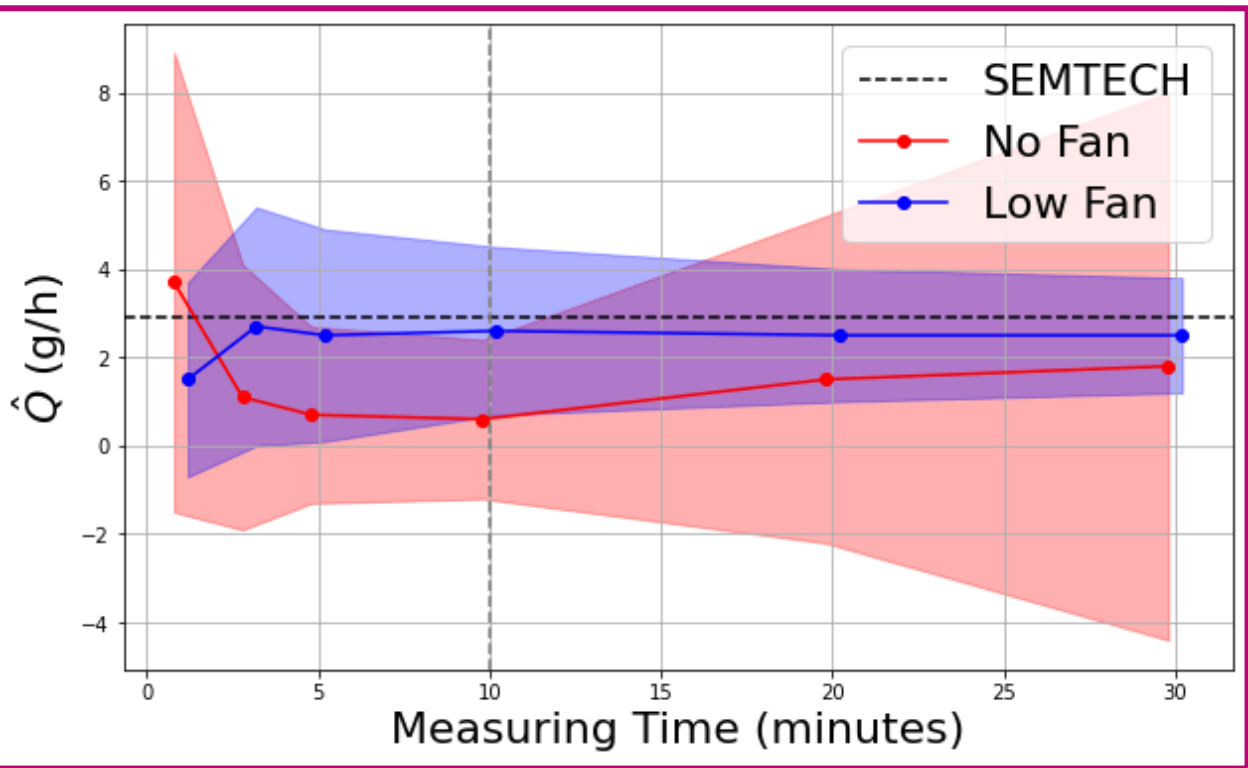
499 **Figure 12**: Estimated leak rates ($\hat{Q}$) and uncertainties ($\sigma_{\hat{Q}}$) from the FAST method for Rayburn #7 as a function of the

500 sampling time used to make the estimate. Without a fan, the measurement is highly uncertain throughout, except for the
501 range from 5-10 minutes. With the fan, the measurement accuracy gets higher with increasing measurement time, but the
502 mean value stays roughly constant above 3 minutes. This shows that the FAST method can be done as quickly as the
503 SEMTECH and accuracy only increases with increased measuring time.
504
505   Figure 12 shows the results of the FAST method at the Low fan (blue) and No fan (red) settings on Rayburn #7,
506 which was measured in 30 minute intervals, as well as the SEMTECH estimate (black dashed line). For the Low fan setting,
507 the SEMTECH value is always within the uncertainty of the FAST method, even if only the first minute of data is used. The
508 mean rate improves when the measuring time is increased to three minutes, but the error bars remain large. For measuring
509 times larger than three minutes, the error bars decrease nearly linearly with increased measuring time, while the mean stays
510 relatively constant. The No Fan results, on the other hand, do not match the SEMTECH well for measuring time shorter than
511 10 minutes. As expected, as the measuring time increases, the mean value of the FAST method for No Fan gradually
512 approaches the SEMTECH, but the error bars also increase over time. This shows that the measuring time for the FAST
513 method, even at the Low Fan measurement, is similar to that of the SEMTECH (on the order of 3 minutes).
514
515   The total cost of the sensors used in this study, a Picarro G4302 for concentration (~40,000 USD) and Gill
516 Windmaster 1210-PK-085 (~5,000 USD) for wind, are about the same cost as a SEMTECH HI-FlOW (~50,000 USD).
517 However, the FAST method can be done without using 3D wind measurements. By replacing the 3D anemometer with a 1D
518 anemometer, the cost of the FAST method can be decreased with minimal loss in accuracy. Effectively, using a 1D
519 anemometer would limit the filter angle to be up to 180 degrees, which has marginally worse accuracy than filtering by 300
520 degrees. Furthermore, the type of methane sensor can be optimized to a more reasonable price point, as CH_4 signals near
521 sources are typically high (e.g., > 1 ppm for leaks > 1 g/h). ~~These levels can be effectively measured using less sensitive and~~
522 ~~more affordable technologies, such as near-infrared (NIR) sensors, non-dispersive infrared (NDIR) sensors, or solid-state~~
523 ~~absorption methods. For example, the MP400 series NDIR Dual Range Methane Sensor [MP400 Series NDIR], available for~~
524 ~~approximately $880, offers dual-range measurement capabilities (1-100% LEL/1-100% Vol), making it a cost-effective~~
525 ~~option. In contrast, the parts-per-billion sensitivity Picarro G4302, while highly precise, has limitations for the FAST method~~
526 ~~due to its low range, saturating above 800 ppm in methane mode. Future work will focus on investigating a wide variety of~~
527 ~~methane detection technologies to identify more cost-effective and reliable solutions for wide-scale FAST method~~
528 ~~deployment. Promising alternatives include portable devices such as the Bascom-Turner Gas-Rover II, designed for efficient~~
529 ~~leak surveys and priced at approximately $4,400 [*VGI-201/211 Gas-Rover II*], or advanced methods like Off-Axis Integrated~~
530 ~~Cavity Output Spectroscopy (ICOS) instruments, such as Nikira Labs' Portable Methane Gas Analyzer, which combines~~
531 ~~sensitivity and portability [Portable Methane Analyzer]~~ Future work will focus on investigating a wide variety of methane
532 detection technologies to identify more cost-effective and reliable solutions for wide-scale FAST method deployment.
533
534   Besides its potential for being lower cost, the FAST method has other advantages over the existing technologies we
535 tested (FLIR and SEMTECH). First, the FLIR camera is insensitive to small leaks and unable to detect most diffuse
536 emissions and is unable to quantify emissions accurately [Zeng and Morris, 2019]. Furthermore, while our existing
537 proof-of-concept FAST hardware is currently heavier and more complex to operate than a SEMTECH, it could be replicated
538 with a battery powered fan mounted to a tripod or a backpack vacuum blower, making it very similar to the size and labor
539 requirements of the SEMTECH. Although both the FAST method and the SEMTECH take approximately three minutes to
540 obtain a measurement, the FAST method currently requires a longer setup time (~30 minutes) compared to the SEMTECH

541 (~5 minutes). ~~However, with the aforementioned simplified setup, the FAST method's setup time could be reduced to match~~
542 ~~that of the SEMTECH, making it more practical for field deployment.¶~~

543
544

5. Conclusions

546
547 ¶
548   We have shown that using a fan to create a forced flow at close range between the emission source and a point
549 methane (CH_4) sensor and measuring 3D wind profiles using a sonic anemometer and CH_4 concentration with a gas analyzer
550 (sampling technique), a simple estimate of the CH_4 emission rate of the source can be inferred (FAST method). The FAST
551 method has been tuned using single, continuous point sources between 0.9 and 37 g/h at 1 m above the ground, in a simple
552 aerodynamic landscape (grass field), in moderate meteorological conditions (< 5 m/s). Under these conditions, the FAST
553 method consistently provided reasonable estimates of leak rates when fan speeds and filtering were applied appropriately,
554 performing similarly to the commercially available method (SEMTECH) and outperforming others (FLIR). Notably, the
555 method's performance improves with increased fan speed and filtering angle. For instance, in the case of Rayburn #7 in
556 Lufkin, Texas, the FAST method at the Low Fan speed consistently produced leak rate estimates that were within the
557 uncertainty bounds of the SEMTECH values after just a few minutes of measurement. Without the use of a fan, the results
558 showed much greater uncertainty, highlighting the importance of airflow in stabilizing methane dispersion for accurate
559 estimation.
560
561   In the Texas and Oklahoma field campaigns, the FAST method ~~was able to provide~~provided accurate and rapid
562 readings under varying environmental conditions, with errors on the order of 95% of the emission rate across ~~a variety~~
563 ~~of~~different wind conditions and leak rates. In Texas, where wind speeds were low, only the Low Fan setting was used, and
564 FAST results aligned closely with SEMTECH, within 10%. ~~Higher wind conditions in Oklahoma, however,~~In Oklahoma,
565 higher wind conditions required both Low and High Fan settings to account for greater natural dispersion. ~~In the case of the~~
566 ~~highly variable Hooper #41, where SEMTECH struggled with the well's fluctuating leak rates, the FAST method's larger~~
567 ~~sampling cross-section and volume resulted in overall lower emissions estimates and relative uncertainty~~At Hooper #41,
568 where emission rates fluctuated significantly, FAST produced lower overall estimates than SEMTECH, likely due to its
569 larger sampling cross-section averaging out short-term variability. However, ~~the~~ fan-driven airflow may not fully entrain all
570 emitted gas, particularly from low-height leaks, ~~potentially leading~~which could contribute to an underestimation of emission
571 rates ~~for such wells.¶~~
572   ¶

573   ~~The FAST method could provide a cost-effective, scalable, and practical~~in certain cases.

574   The FAST method offers a potential alternative to existing technologies such as SEMTECH and FLIR for
575 identifying high-priority orphan wells. ~~The~~Its combination of ~~fan-induced plume dispersion~~controlled airflow and real-time
576 methane measurement ~~allows for quick assessments (on the order of minutes), making it well-suited for large-scale~~
577 ~~monitoring. Future developments in sensor optimization, including the use of more affordable wind and methane detectors,~~
578 ~~are expected to further enhance its deployment efficiency and accuracy across diverse field conditions. Further testing is~~
579 ~~being done to optimize the necessary wind and methane sensors to lower costs and maintain accuracy in order to deploy this~~
580 ~~technology across the U.S. to quantify fugitive emissions.¶~~

581   enables rapid assessments suitable for large-scale monitoring. Ongoing research aims to refine wind and methane
582 sensor integration to improve cost efficiency while maintaining measurement accuracy across diverse field conditions and
583 leak rates.

584

585 Appendix A: Comparison to Gaussian Plume Method

586   The approach to deriving the equations governing the FAST method outlined in the "Mathematical Model" section
587 can also be compared to the more traditional approach using a Gaussian Plume model (GPM). Through this comparison, we
588 can gain deeper insight into the physical significance of the proportionality constant (β), as it relates to the diffusivity of the
589 pollutant of interest. Including a term for reflection from the ground (but not from an inversion aloft), the GPM estimates the
590 downwind concentration of a pollutant as a function of the emission rate (Q), advective velocity (u), crosswind distance from
591 centerline (y), vertical displacement from centerline (z), height of the emission source (H) and horizontal and vertical
592 dispersion coefficients (σ_y σ_z) as follows:

593 $$C(x, y, z) \ = \ \frac{Q}{2\pi\, \sigma_y\, \sigma_z\, u} \, exp\{\frac{-y^2}{2\sigma_y^{\,2}}\}(exp\{\frac{-(z-H)^2}{2\sigma_z^{\,2}}\} \ + \ exp\{\frac{-(z+H)^2}{2\sigma_z^{\,2}}\}) \qquad\qquad (A1)$$

594

595   Similar to the FAST model, the GPM assumes that the velocity profile is constant in space. However, the GPM does
596 not assume the concentration profile is constant, which is implicitly done by the FAST method via the use of centerline
597 time-averaged concentrations (Figure A1). Rather, the GPM assumes that the concentration profiles are Gaussian in the y
598 and z directions, with standard deviations (σ_y, σ_z) related to the width of the plume. These standard deviations are often
599 approximated using empirical data (i.e. Pasquill stability classes) but can be defined exactly using the diffusivity of the
600 pollutant (D). Assuming that the plume is isotropic and homogeneous, we can define:

601 $$\sigma_y \approx \sigma_z \approx \hat{\sigma} \ = \ \sqrt{\frac{2Dx}{u}} \qquad\qquad\qquad (A2)$$

602 where D is the diffusivity of the pollutant and $\hat{\sigma}$ is the standard deviation of the Gaussian plume in all directions orthogonal
603 to x. Evaluating this equation at some downwind distance x_0 and substituting our earlier use of centerline velocity
604 measurements (given that the velocity profile is assumed constant in both GPM and FAST), we can define the standard
605 deviation there ($\hat{\sigma}_0$):

606 $$\hat{\sigma}_0 \ \approx \ \sqrt{\frac{2Dx_0}{u_{CL}}} \qquad\qquad\qquad (A3)$$

607

608 Using this standard deviation, we can imagine integrating the FAST approach over a certain number of standard deviations to
609 capture more and more of the true concentration profile. To capture 99.7% of the total plume, we would need to integrate out

610 to three standard deviations, or $3\hat{\sigma}_0$. Using this comparison to the previous equation derived for FAST (Equation 2), we can

611 solve for β.

612

$$\sigma_0 = \sqrt{\beta\, i_{fan}\, l_{fan}\, x_0} \simeq 3\hat{\sigma}_0 \approx 3\sqrt{\frac{2Dx_0}{u_{CL}}}$$

614   (A4)

615 $$\beta \approx \frac{18\, D}{i_{fan}\, l_{fan}\, u_{CL}}$$ (A5)

616

617 Here, we find that the proportionality constant β can be understood as a non-dimensional ratio of two diffusivities - one

618 being the true diffusivity of the gas and the other being due to the turbulence generated by the fan. Since D can be very

619 difficult to measure, the FAST method provides a work-around such that only constants related to the fan-generated flow

620 need to be defined to quantify the emission rate. Equation A5 could also be inverted to estimate the diffusivity D, but this is

621 not of real interest for this study

622

623
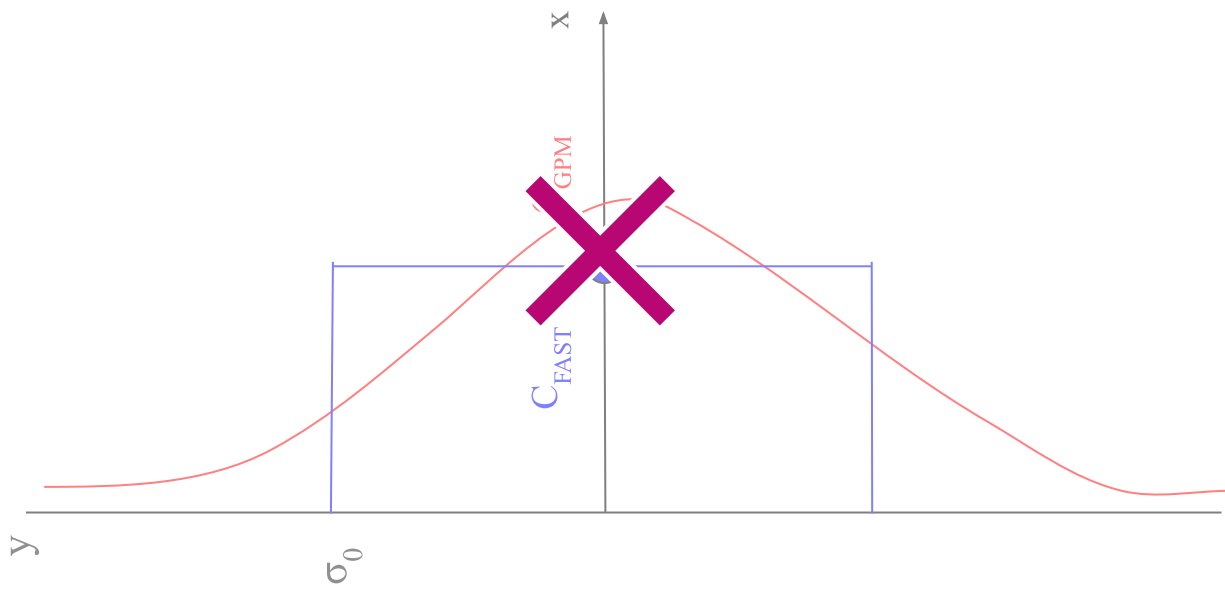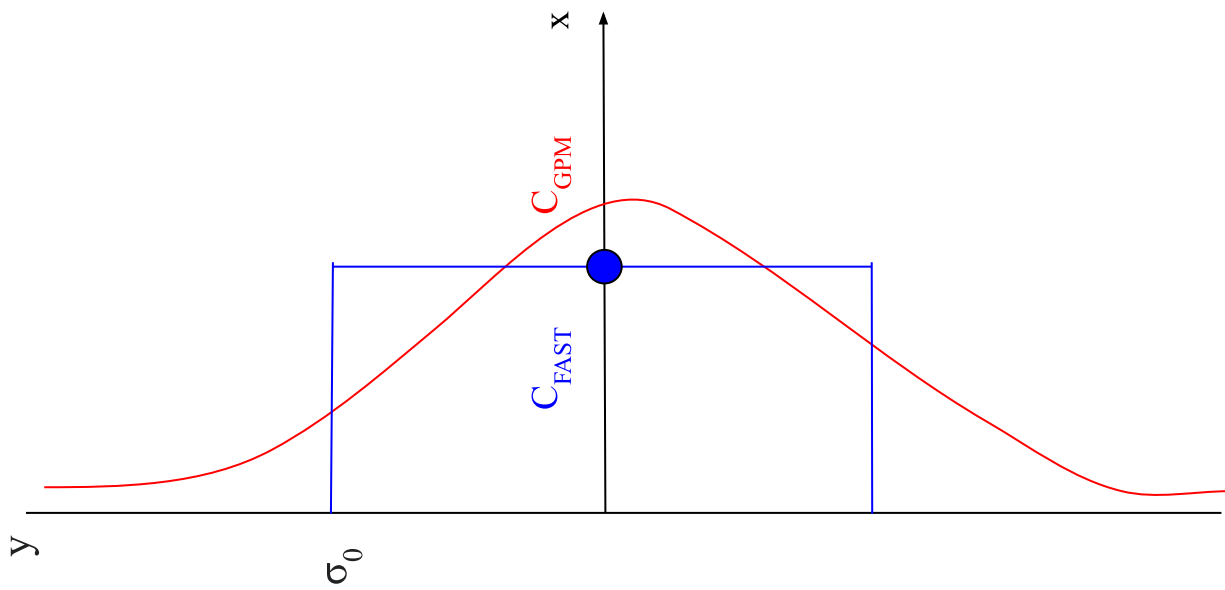
Figure A1: Diagram showing the difference in concentration profiles (C) used by the FAST (blue) and GPM (red) methods

We also calculated the estimated emissions from a Gaussian Plume Model (GPM) using three different Pasquill Stability Classes (A, B and C) based on the no fan concentration and wind measurements for each well (shown in the table below). As evidenced by the order of magnitude range for each well, the GPM is highly sensitive to the choice of stability class, which is not immediately apparent for such short range measurements. We used the equations for calculating σ_y and σ_z from [Cooper and Alley, 2011, pp. 662-663].

Date	Well ID	SEMTECH (g/hr)	FAST (300 Filter) (g/hr)	GPM for Daytime Pasquill Stability Classes (g/hr)
2024-02-06	Rayburn #7 (Lufkin)	2.9 ± 0.0	Low: 2.6 ± 1.9 No: 0.6 ± 1.8	Class A: 3.41 ± 20.2 Class B: 0.87 ± 5.18 Class C: 0.01 ± 0.08
2024-02-07	Undisclosed Well (Lufkin)	1.0 ± 0.3	Low: 0.5 ± 0.7 No: 1.3 ± 3.4	Class A: 1.05 ± 13.5 Class B: 0.27 ± 3.45 Class C: 0.0 ± 0.0
2024-03-14	Humphrey #5 (Barnsdall)	2.0 ± 0.04	High: 2.0 ± 1.1 Low: 2.5 ± 1.5 No: 10.0 ± 15.1	Class A: 226 ± 336 Class B: 57.8 ± 85.8 Class C: 1.06 ± 1.57
2024-03-14	Hooper #41 (Barnsdall)	70.1 ± 95.5	High: 9.3 ± 10.4 Low: 9.9 ± 12.7 No: 1.0 ± 4.0	Class A: 70.0 ± 332 Class B: 17.8 ± 84.2 Class C: 0.0 ± 0.0

Table A1: Estimated leak rates ($\hat{Q}$) and uncertainties ($\sigma_{\hat{Q}}$) for the four wells shown in Figure 6 from the SEMTECH, FAST method (filtered) and a Gaussian Plume Model (GPM) for all possible daytime Pasquill Stability Classes.

Based on there being moderate to strong insolation and low wind speeds (<2 m/s) for the Texas wells, the most likely stability class for Rayburn #7 and Undisclosed Well is Class A or B. Using these stability classes, the GPM does reasonably well at estimating the magnitude of the leak but the uncertainty is much higher than both the SEMTECH and the FAST method. Due to the higher background wind speeds (3-5 m/s) and moderate to strong insolation in Oklahoma, the B and C stability classes are most likely for Humphrey #5 and Hooper #41. Here, the GPM overestimates the magnitude of Humphrey #5 by orders of magnitude and the uncertainty is very high. For Hooper #41, which is a highly variable well, the GPM also still performs poorly relative to the SEMTECH and FAST methods.

Appendix B: SEMTECH Measurements

648

649   The SEMTECH Hi-Flow 2 is a methane emission quantification system composed of a backpack-mounted gas
650 analyzer and a long sampling inlet tube with a fan to sample the methane emitted by a point source. This system reports the
651 flow of methane emitted in liters per minute (LPM) in a range of 0.02 LPM to 730 LPM (1 g/hour - 29 kg/hour) (0.001 CFM
652 to ~25 CFM), with an accuracy of ~10% [SEMTECH].
653

654   The measurement principle of the SEMTECH HI-FLOW relies on simultaneous measurements of air flow and
655 methane concentration. If F_{air} is the volumetric flow rate of air captured by the system (in LPM), C is the concentration of
656 methane in ppm, $C_{background}$ is the concentration of methane of the background, and $K(T,P,\eta)$ an adjustment parameter varying
657 with temperature (T), pressure (P), air viscosity(η), then we can express the volumetric flow rate of methane F_{CH4} as:
658

659        $F_{CH4} = F_{air} \bullet (C - C_{background}) \bullet K(T,P,\eta)$ (B1)
660

661   The velocity of the air is measured using a pitot tube, and the concentration of methane is measured using a gas
662 analyzer (near-IR laser absorption CH_4 sensor sensitive on a range of 10 ppm to 100% of CH_4) located in the backpack. All
663 other parameters such as temperature and pressure are also measured by the SEMTECH directly in the pitot tube. This
664 system is designed to be user friendly, as the flow measured is directly shown on the system monitor. Data are logged every
665 second (1Hz). For example as we can see in Figures B1 and B2, the SEMTECH measures the CH_4 emission rate, at a rate of
666 one point per second, and returns a value in liters per minute (LPM) which we converted to g/h for more convenient use.
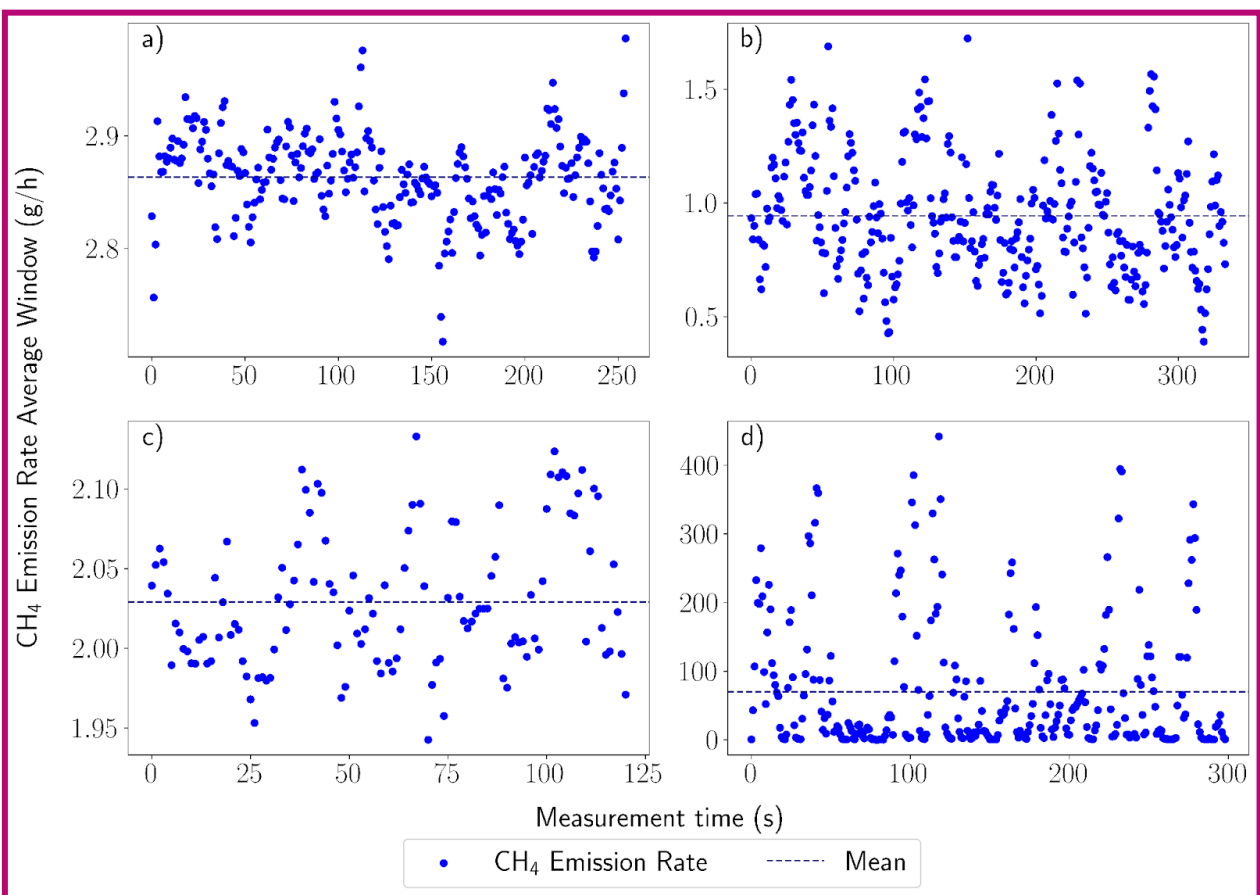667

43

a) 0.96 ± 0.03 g/h

b) 1.89 ± 0.05 g/h

c) 4.62 ± 0.08 g/h

d) 9.25 ± 0.16 g/h

e) 18.3 ± 0.33 g/h

f) 36.9 ± 0.53 g/h

CH$_4$ Emission Rate Average Window (g/h)

Measurement time (s)

CH$_4$ Emission Rate   Mean   Mean ± Std Dev

Figure B1: Left to right and top to bottom, shows the increasing steps measurements of controlled release emission rates from the SEMTECH. As the control release flow rate increases, the accuracy and precision of the SEMTECH decrease.

Figure B2: SEMTECH HI-FLOW measurements (time series and mean) from the four orphaned wells used in the FAST method validation.

Appendix C: Fan Characterization Results

a Wind Speed (u, v, w)

b Standard Deviation of Wind Direction (y, z)
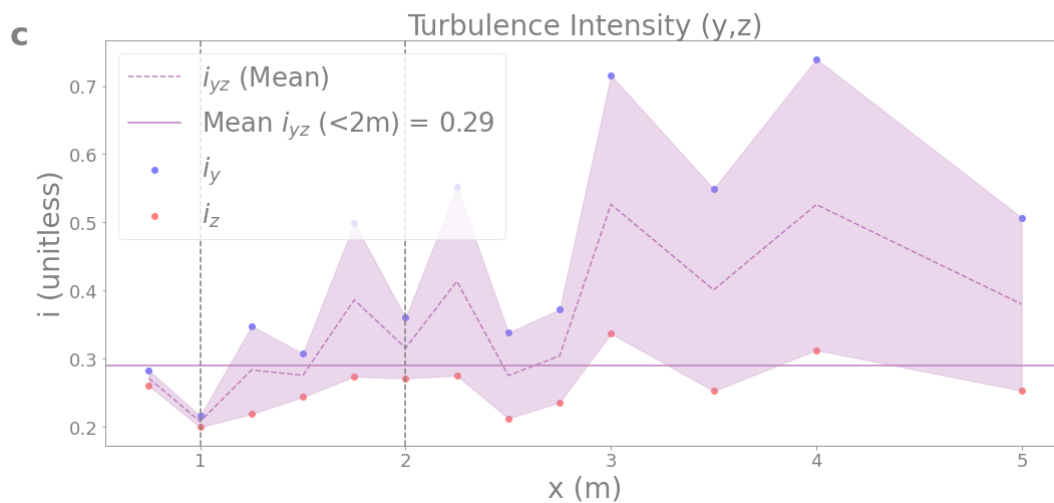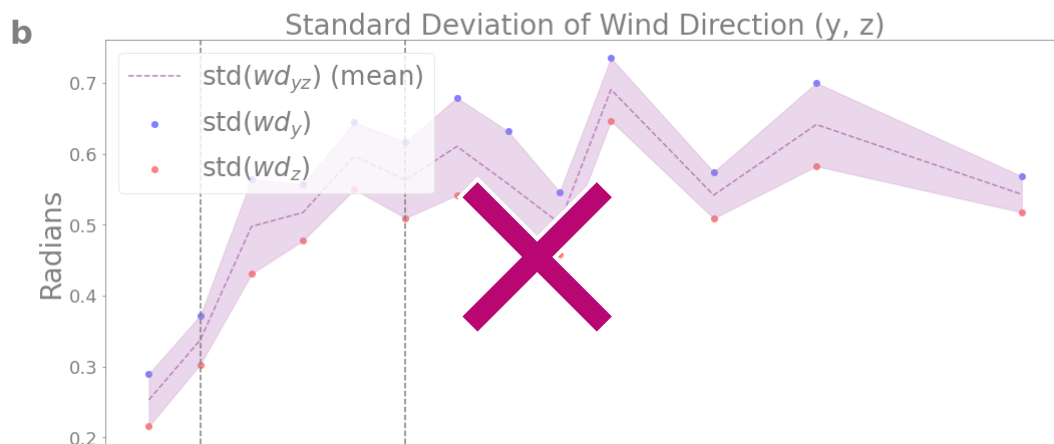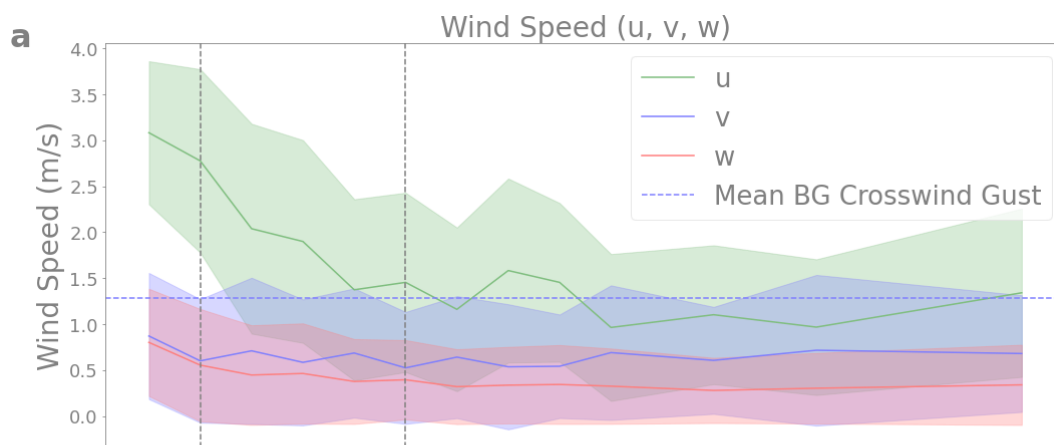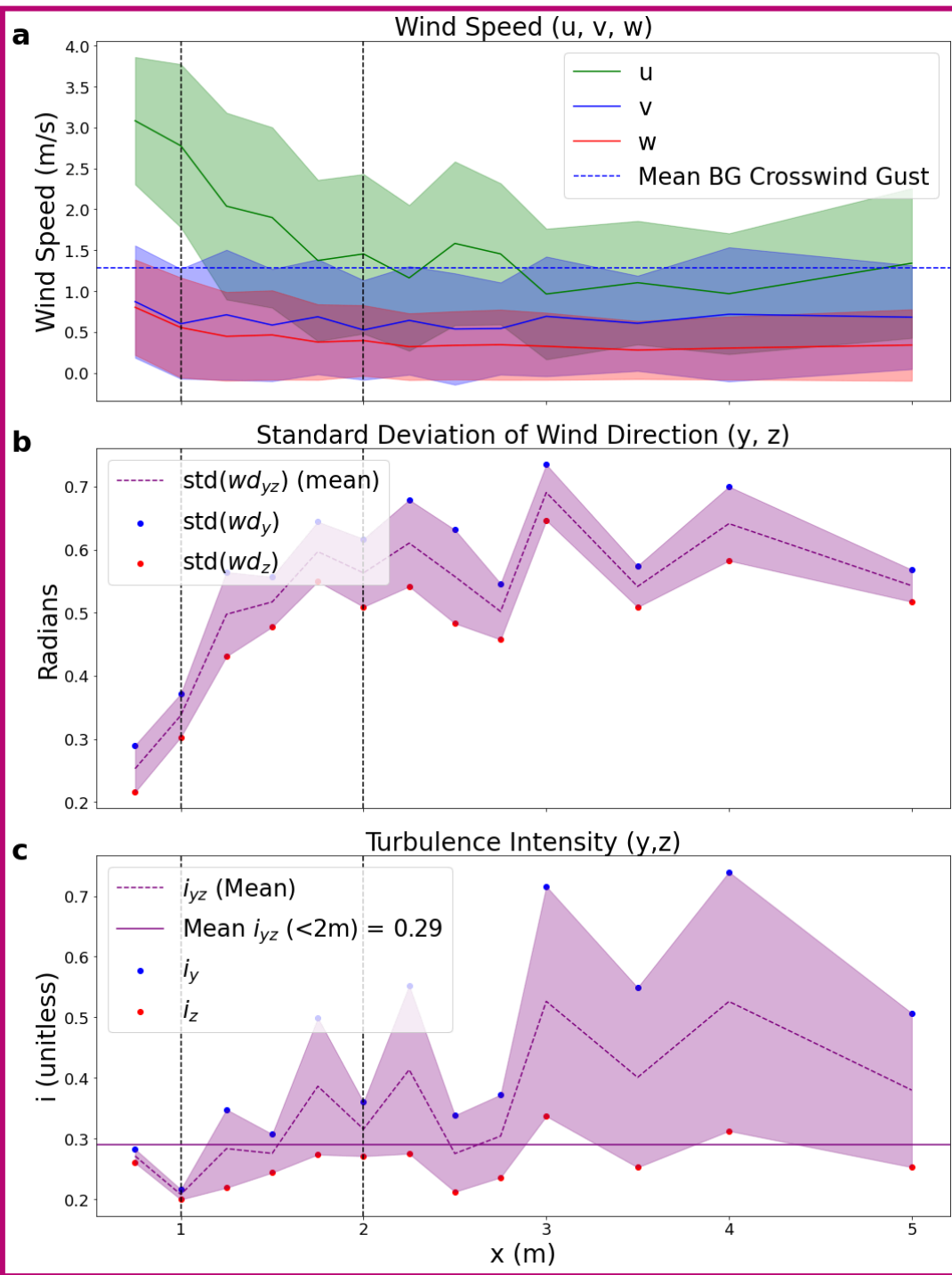
c Turbulence Intensity (y,z)

Figure C1: a) Wind speed, b) standard deviation of wind direction, and c) turbulence intensity as a function of downwind distance x for Experiment 1 using the Low fan speed setting. Data are filtered to remove any points coming from the negative x direction (180 degrees)

49
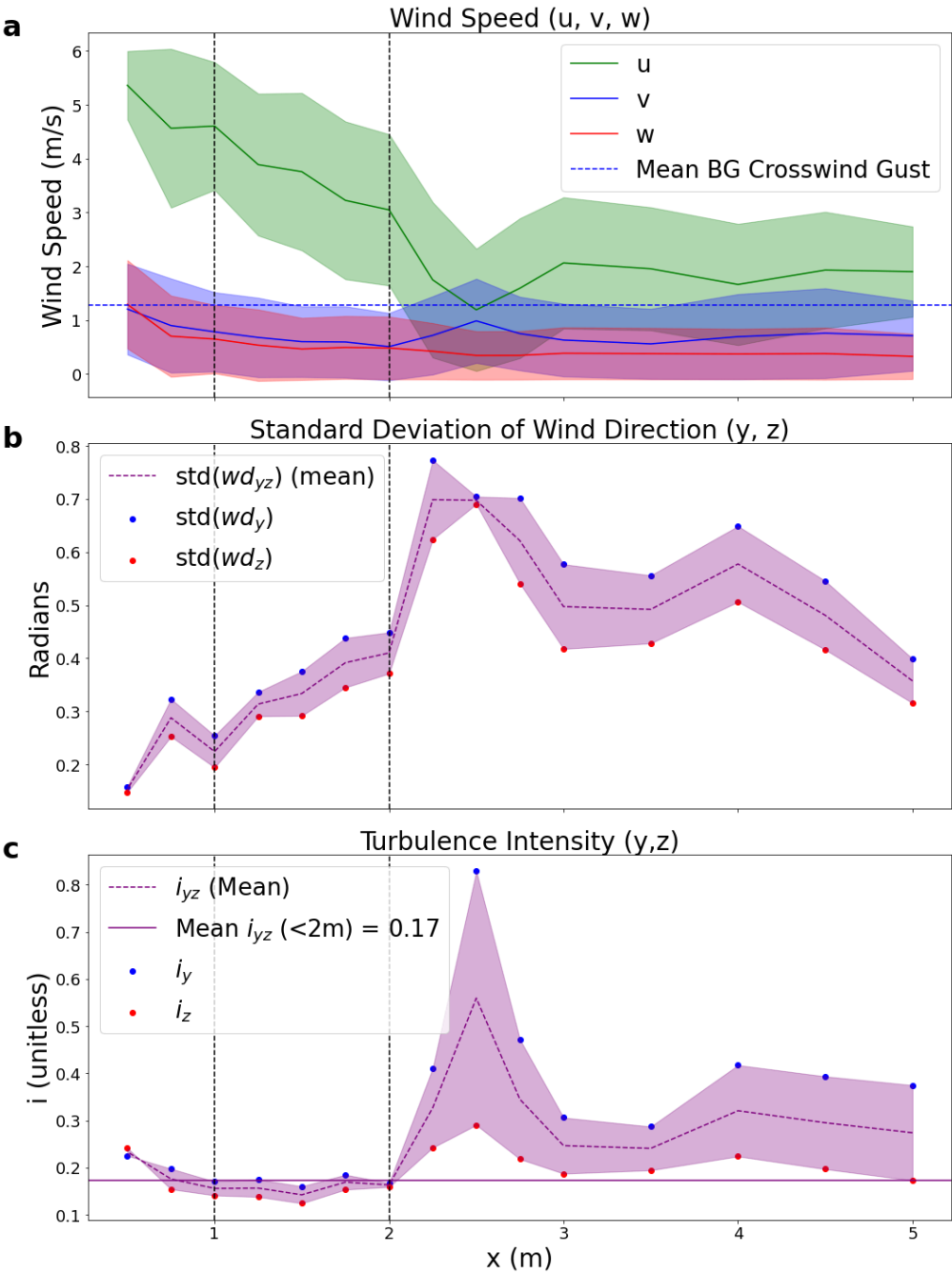
Figure C2: a) Wind speed, b) standard deviation of wind direction, and c) turbulence intensity of Experiment 1 using the High fan speed setting. Data are filtered to remove any points coming from the negative x direction (180 degrees)
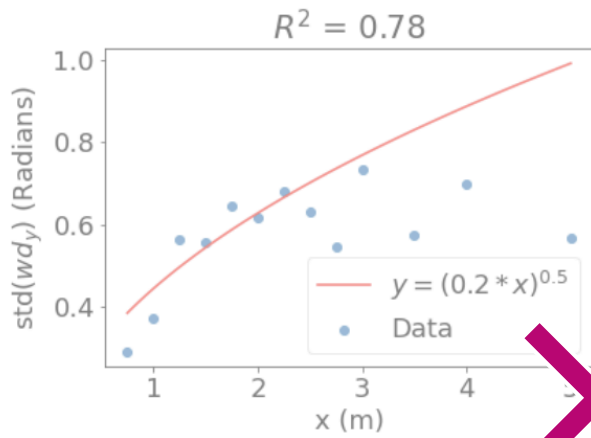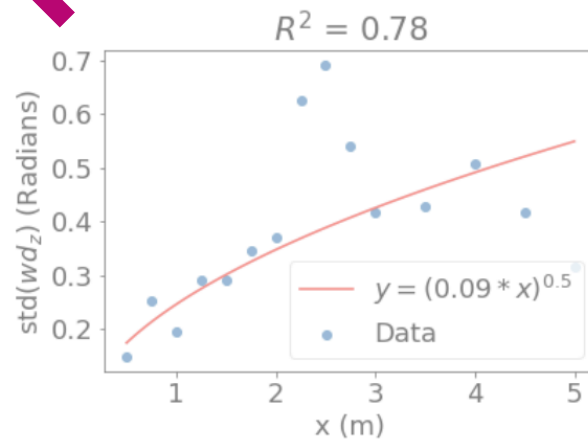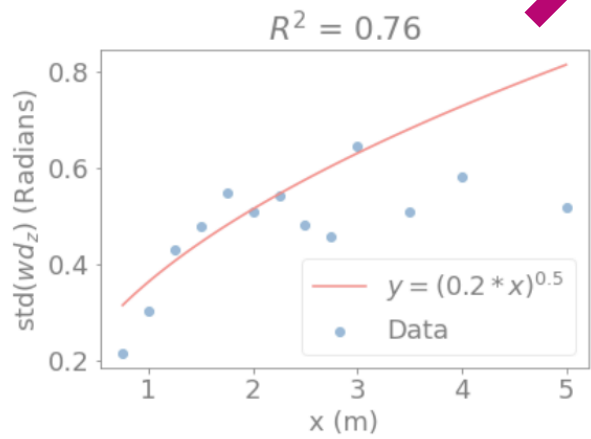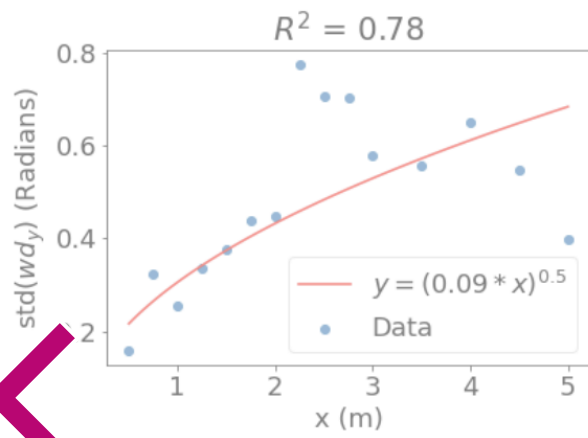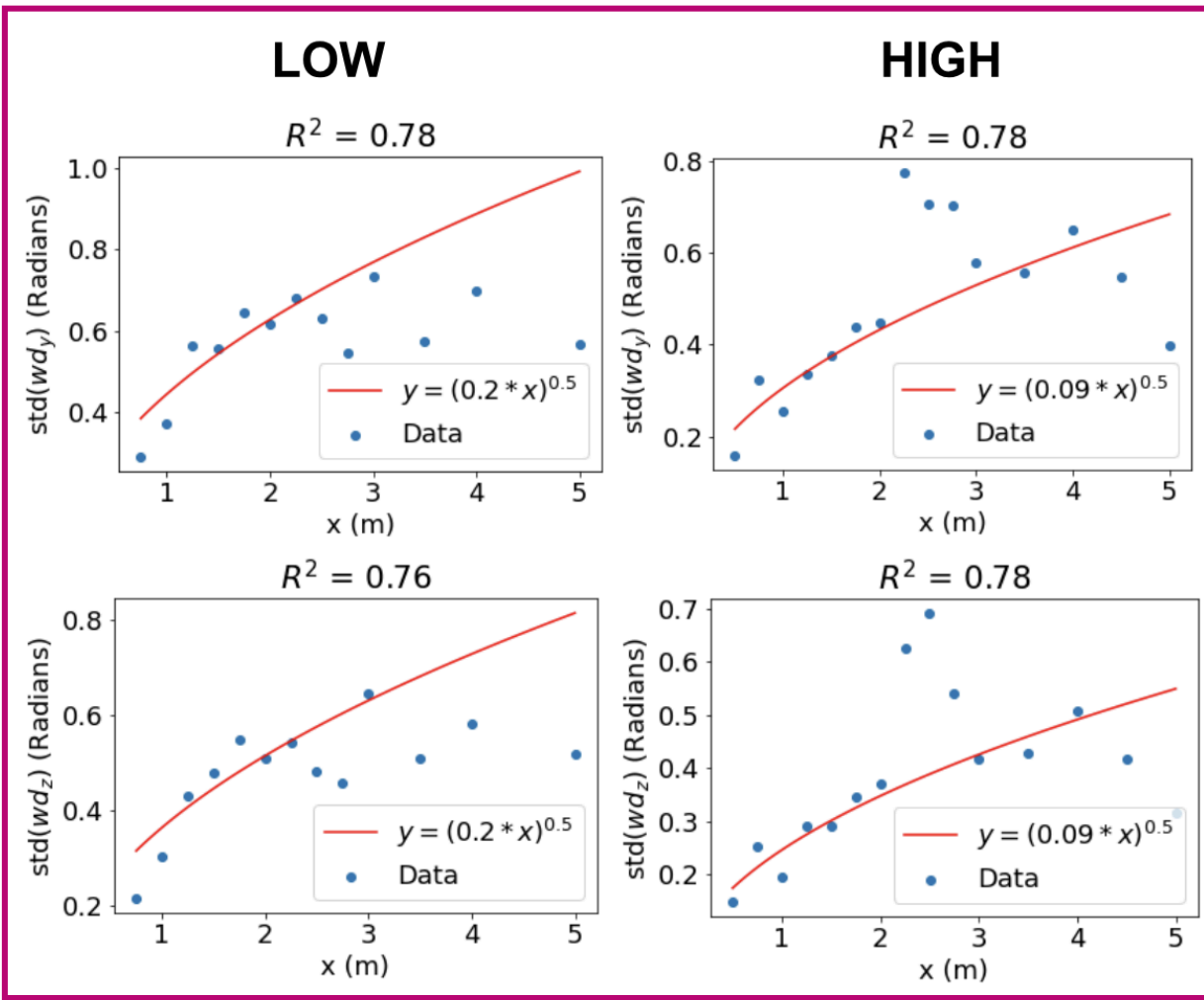
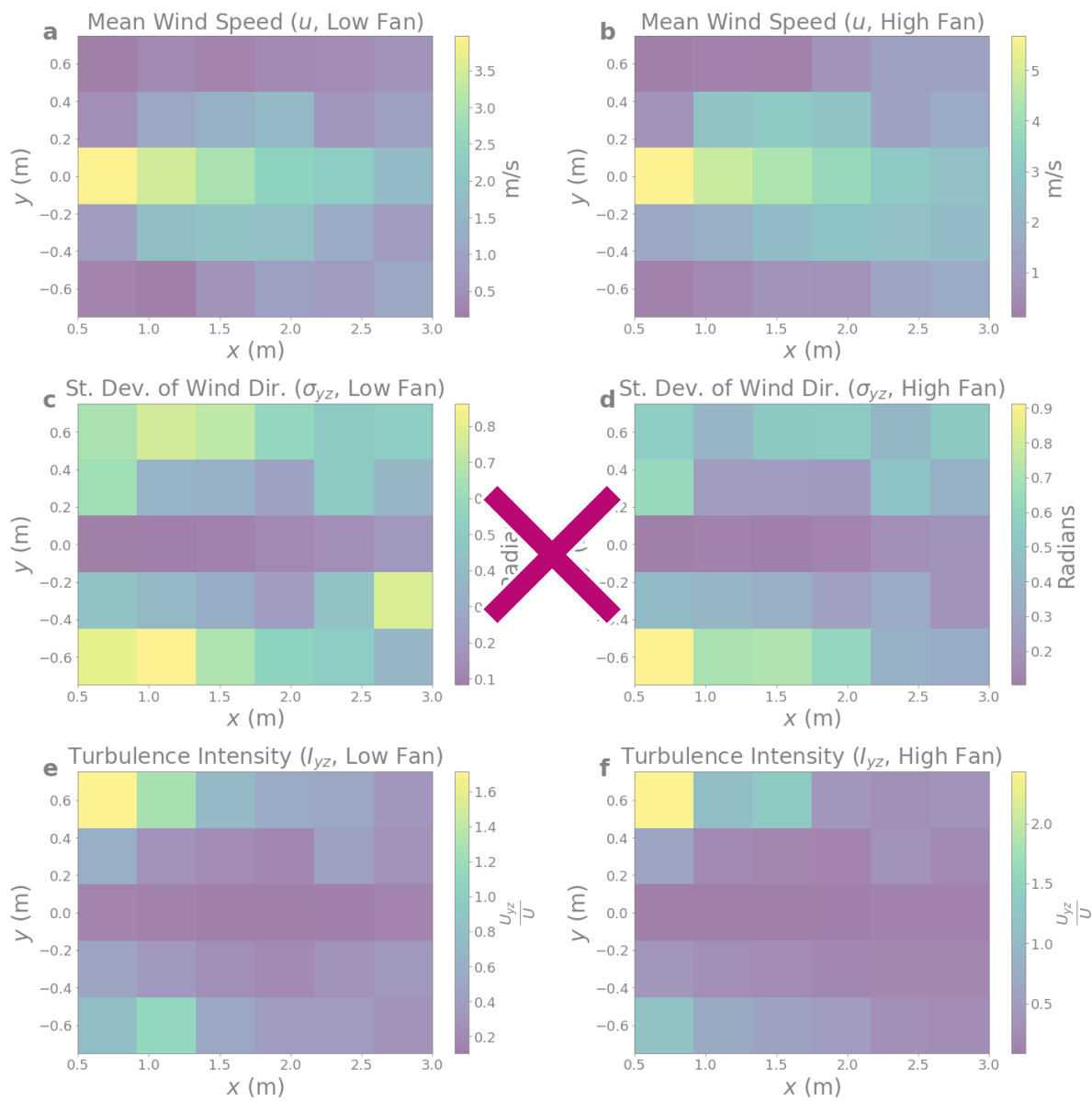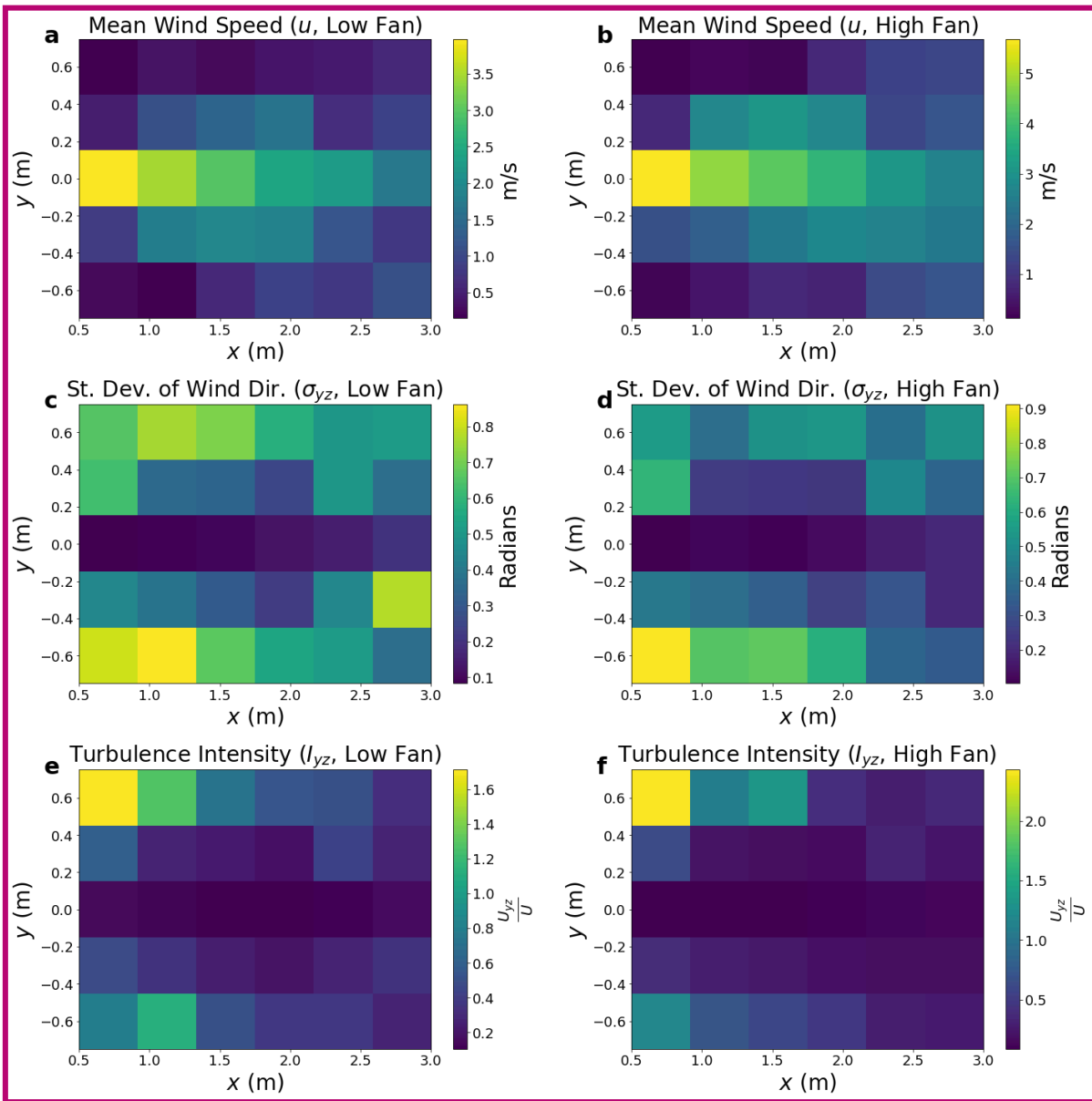**Figure C3**: Square root fits to the standard deviations (std) of wind direction with filter angle = 180 degrees as expected by equation 2. The fits are valid in the range of 1-2 meters and depart from the square-root curve at larger downwind distances.

The results of the first fan characterization experiment are summarized in Figures C1-3. Figures C1 and C2 show the mean wind speed in 3D (u, v, w), standard deviation of wind direction in the x-y (std(wd_y)) and x-z (std(wd_z)) planes and turbulence intensity in the y (i_y) and z (i_z) directions at the range of downwind distances (x) for the Low and High fan speeds respectively. For both fan speeds, the u component of the flow starts higher than the background and decreases nearly linearly with distance until it is on the same order of magnitude as the background crosswind gust intensity (blue dashed line). The std(wd_y) and std(wd_z) values are calculated using the Yamartino method [Turner, 1986] and act as an estimate of the effective width of the plume (in radians). According to Equation 2, these should both therefore grow proportional to $x^{0.5}$, which is verified for x < 2 meters in Figure C3. The turbulence intensities (i_y) and (i_z) are calculated using the means of the magnitudes of u, v and w as mean(v)/mean(u) and mean(w)/mean(u) respectively. These should be relatively constant for the fan generated flow (i_{fan}) and about equal if the turbulence of the flow is uniform. The uniform flow near the fan is much more evident in the High fan data (Figure C2), whereas the Low fan measurements (Figure C1) indicate the effects of crosswind turbulence, resulting in much larger values of i_y compared to i_z. It is also important to note that during the measurement

52

period for the High fan speed, the crosswinds far exceeded their background value, resulting in a total disruption of the plume in this region (2 m < x < 3 m). The crosswinds died down later in the experiment when the anemometer was further downwind, resulting in a more stable plume for x > 3 m. Overall, we found that the fan plume remained stable to a wide range of crosswind conditions in the range of 1 m < x < 2 m.

a Mean Wind Speed (u, Low Fan)

b Mean Wind Speed (u, High Fan)

c St. Dev. of Wind Dir. (σ_{yz}, Low Fan)

d St. Dev. of Wind Dir. (σ_{yz}, High Fan)

e Turbulence Intensity (I_{yz}, Low Fan)

f Turbulence Intensity (I_{yz}, High Fan)

712

54

Figure C4: a-b) Mean wind speed, c-d) standard deviation of wind direction in the x-y plane, and e-f) turbulence intensity in the y-z plane of Experiment 2 for low-fan setting (left) and high-fan setting (right).

The results of the second fan characterization experiment are summarized in Figure C4. Similar to Figure C1, the top row shows the mean wind speed in the downwind direction (u), the mean of standard deviation of wind direction in the x-y (std(wd_y)) and x-z (std(wd_z)) planes, and the mean of the turbulence intensity in the y (i_y) and z (i_z) directions at a range of downwind distances (x) and crosswind distances (y) for the Low and High fan speeds (left and right, respectively). Unlike the first experiment, these measurements allowed for variation in both x and y, allowing us to investigate the shape of the plume. The experiment was done with very little background wind (before sunrise) and in a location shielded from crosswind

723 on one side by a wall (Fig. 2). The measurements were taken at 10 Hz for 1 minute intervals at each of the points in the x-y
724 grid (0.5 m intervals in x for $0.5 < x < 3.0$ and 0.33 m intervals in y for $-0.66 < y < 0.66$) as depicted in Figure C4.
725

726   From these measurements, the MDB fan was able to generate a jet of pseudo-homogeneous turbulence at a range of
727 downwind distances between 1 and 2 meters. Beyond 2 meters, the plume becomes unstable and can be broken easily by
728 crosswinds, even at a High fan setting. Furthermore, the heat maps in Figure C4 also point to the importance of measuring
729 along the centerline ($y = 0$), as the effects of crosswind turbulence increase by a large amount even when only slightly off of
730 the centerline ($y > 0.3$ m). Based on these results, the controlled release experiment was conducted with the sensors at a
731 distance of 2 meters from the fan, and all of the field measurements were performed with a distance of less than 2 meters.
732

733

734

735 **Author contribution**:

736 Mohit L. Dubey: Conceptualization, Data curation, Formal analysis, Investigation, Methodology, Software, Validation,
737 Visualization, Writing

738 Andre Santos: Conceptualization, Data curation, Investigation, Methodology, Validation, Visualization, Writing

739 Andrew B. Moyes: Conceptualization, Investigation, Methodology, Validation, Writing (review and editing)

740 Ken Reichl: Conceptualization, Data curation, Investigation, Methodology, Validation, Writing

741 James E. Lee: Investigation, Writing (review and editing)

742 Manvendra K. Dubey: Investigation, Writing (review and editing)

743 Corentin LeYhuelic: Investigation, Formal analysis, Writing (review and editing)

744 Evan Variano: Formal analysis

745 Emily Follansbee: Investigation, Writing (review and editing)

746 Fotini K. Chow: Conceptualization, Formal analysis, Writing (review and editing)

747 Sébastien C. Biraud: Conceptualization, Investigation, Methodology, Validation, Writing (review and editing), Project
748 administration, Funding acquisition

749

750 **Competing interests**:

751 The authors declare that they have no conflict of interest.

References

Cooper, C. D., and F. C. Alley. *Air Pollution Control: A Design Approach*. 4th ed., Waveland Press, Inc., 2011.

DOI. *Biden-Harris Administration Invests $660 Million for States to Plug Orphaned Oil and Gas Wells through President's Investing in America Agenda | U.S. Department of the Interior*. 10 July 2023, https://www.doi.gov/pressreleases/biden-harris-administration-invests-660-million-states-plug-orphaned-oil-and-gas-wells

Dooley, Jonathan F., et al. *A New Technique for Airborne Measurements to Quantify Methane Emissions Over a Wide Range: Implementation and Validation*. 19 Mar. 2024, https://doi.org/10.5194/egusphere-2024-760.

Dubey, Manvendra, et al. *How to Estimate O&G Well Leak Rates from near Field Concentration and Wind Observations?* LA-UR-23-20659, 1922013, 4 Apr. 2023, p. LA-UR-23-20659, 1922013, https://doi.org/10.2172/1922013.

Edie, Rachel, et al. "Constraining the Accuracy of Flux Estimates Using OTM 33A." *Atmospheric Measurement Techniques*, vol. 13, no. 1, Jan. 2020, pp. 341–53, https://doi.org/10.5194/amt-13-341-2020.

Follansbee, Emily, et al. *Quantifying Methane Fluxes from Super-Emitting Orphan Wells to Report Carbon Credits and Prioritize Remediation*. 8 June 2024, https://doi.org/10.22541/essoar.171781163.39594276/v1.

GasScouterTM G4302 Mobile Gas Concentration Analyzer | Picarro. https://www.picarro.com/environmental/products/gasscoutertm_g4302_mobile_gas_concentration_analyzer. Accessed 7 Jan. 2025.

Halloran, Siobhan K., et al. "Turbulent Dispersion via Fan-Generated Flows." *Physics of Fluids*, vol. 26, no. 5, May 2014, p. 055114, https://doi.org/10.1063/1.4879256.

IEA. "Methane Tracker 2020 – Analysis." *IEA*, 30 Mar. 2020, https://www.iea.org/reports/methane-tracker-2020.

IOGCC. *IDLE AND ORPHAN OIL AND GAS WELLS: STATE AND PROVINCIAL REGULATORY STRATEGIES*. 2021, https://iogcc.ok.gov/sites/g/files/gmc836/f/documents/2022/iogcc_idle_and_orphan_wells_2021_final_web_0.pdf.

Kang, Mary, et al. "Environmental Risks and Opportunities of Orphaned Oil and Gas Wells in the United States."

Environmental Research Letters, vol. 18, no. 7, July 2023, p. 074012, https://doi.org/10.1088/1748-9326/acdae7.

Lushi, Enkeleida, and John M. Stockie. "An Inverse Gaussian Plume Approach for Estimating Atmospheric Pollutant

Emissions from Multiple Point Sources." *Atmospheric Environment*, vol. 44, no. 8, 2010, pp. 1097–107,

https://doi.org/10.1016/j.atmosenv.2009.11.039.

Merrill, Matthew D., et al. *Analysis of the United States Documented Unplugged Orphaned Oil and Gas Well Dataset*.

1167, U.S. Geological Survey, 2023, https://doi.org/10.3133/dr1167.

~~"MP400 Series NDIR Dual Range Methane 1-100 %LEL/1-100 %Vol Sensor." *MPower Electronics, Inc*,~~

~~https://shop.mpowerinc.com/products/mp400-series-ndir-dual-range-methane-1-100-lel-1-100-vol-sensor. Accessed 9 Jan.~~

~~2025.~~

Perry, Steven G., et al. "AERMOD: A Dispersion Model for Industrial Source Applications. Part II: Model Performance

against 17 Field Study Databases." *Journal of Applied Meteorology*, vol. 44, no. 5, May 2005, pp. 694–708,

https://doi.org/10.1175/JAM2228.1.

~~"Portable Methane Analyzer." *Nikira Labs*, https://www.nikiralabs.com/portable-methane-gas-analyzer. Accessed 9 Jan.~~

~~2025.~~

Porter, J. G., et al. *Eddy Flux Measurements of Sulfur Dioxide Deposition to the Sea Surface*. 13 June 2018,

https://doi.org/https://doi.org/10.5194/acp-18-15291-2018. Atmos. Chem. Phys. Discuss.

Riddick, Stuart N., Riley Ancona, Mercy Mbua, Clay S. Bell, et al. "A Quantitative Comparison of Methods Used to

Measure Smaller Methane Emissions Typically Observed from Superannuated Oil and Gas Infrastructure." *Atmospheric

Measurement Techniques*, vol. 15, no. 21, Nov. 2022, pp. 6285–96, https://doi.org/10.5194/amt-15-6285-2022.

Riddick, Stuart N., Mercy Mbua, Arthur Santos, et al. "Methane Emissions from Abandoned Oil and Gas Wells in

Colorado." *Science of The Total Environment*, vol. 922, 2024, p. 170990, https://doi.org/10.1016/j.scitotenv.2024.170990.

Riddick, Stuart N., Mercy Mbua, John C. Riddick, et al. "Uncertainty Quantification of Methods Used to Measure

Methane Emissions of 1 g CH4 H−1." *Sensors*, vol. 23, no. 22, Nov. 2023, p. 9246, https://doi.org/10.3390/s23229246.

Riddick, Stuart N., Denise L. Mauzerall, Michael A. Celia, Mary Kang, et al. "Variability Observed over Time in Methane Emissions from Abandoned Oil and Gas Wells." *International Journal of Greenhouse Gas Control*, vol. 100, 2020, p. 103116, https://doi.org/10.1016/j.ijggc.2020.103116.

Saint-Vincent, Patricia M. B., et al. "An Analysis of Abandoned Oil Well Characteristics Affecting Methane Emissions Estimates in the Cherokee Platform in Eastern Oklahoma." *Geophysical Research Letters*, vol. 47, no. 23, Dec. 2020, p. e2020GL089663, https://doi.org/10.1029/2020GL089663.

Sánchez-Sosa, Jorge Edwin, et al. "An Application of the Gaussian Plume Model to Localization of an Indoor Gas Source with a Mobile Robot." *Sensors (Basel, Switzerland)*, vol. 18, no. 12, Dec. 2018, p. 4375, https://doi.org/10.3390/s18124375.

SEMTECH. *SEMTECH HI-FLOW 2*. 2024, https://sensors-inc.com/Products/Custom_Solutions/SEMTECH_HI-FLOW_2.

Sherwin, Evan D., et al. "US Oil and Gas System Emissions from Nearly One Million Aerial Site Measurements." *Nature*, vol. 627, no. 8003, Mar. 2024, pp. 328–34, https://doi.org/10.1038/s41586-024-07117-5.

Snoun, Hosni, et al. "A Comprehensive Review of Gaussian Atmospheric Dispersion Models: Current Usage and Future Perspectives." *Euro-Mediterranean Journal for Environmental Integration*, vol. 8, no. 1, 2023, pp. 219–42, https://doi.org/10.1007/s41207-023-00354-6.

Taylor, G. I. "Diffusion by Continuous Movements." *Proceedings of the London Mathematical Society*, vol. s2-20, no. 1, 1922, pp. 196–212, https://doi.org/10.1112/plms/s2-20.1.196.

UNFCCC Secretariat. *UN Climate Change Global Innovation Hub COP26 Event Report*. 1 Mar. 2022, https://unfccc.int/documents/460986.

U.S. EPA. *Other Test Method – 34: Method to Quantify Road Dust Particulate Matter Emissions(PM10 and/or PM2.5) from Vehicular Travel on Paved and Unpaved Roads*. 2014.

Veigele, Wm. J., and James H. Head. "Derivation of the Gaussian Plume Model." *Journal of the Air Pollution Control Association*, vol. 28, no. 11, 1978, pp. 1139–40, https://doi.org/10.1080/00022470.1978.10470720.

Ventbusters. "Achieve Net-Zero with Ventsentinel®: Revolutionizing Methane Emission Monitoring." *Ventbusters*, 10 Nov. 2023, https://www.ventbusters.com/updates/2023/11/10/greenhouse-gas-emission-monitoring-with-the-ventsentinel-a-revolutionary-advanvcement-in-continuous-vent-gas-quantification.

VGI-201/211 Gas-Rover II Natural Gas Detector [2022] - $4,400.00 : Bascom-Turner Store - Portable Gas Detectors. https://www.bascom-turner.com/store/index.php?main_page=product_info&products_id=462. Accessed 9 Jan. 2025.